REVIEW

Macromolecular Materials and Engineering

www.mame-journal.de

Advances in Electrospun Fiber-Based Flexible Nanogenerators for Wearable Applications

*Tugce A. Arica, Tugba Isık, Tugrul Guner, Nesrin Horzum, and Mustafa M. Demir**

In today's digital age, the need and interest in personal and portable electronics shows a dramatic growth trend in daily life parallel to the developments in sensors technologies and the internet. Wearable electronics that can be attached to clothing, accessories, and the human body are one of the most promising subfields. The energy requirement for the devices considering the reduction in device sizes and the necessity of being flexible and light, the existing batteries are insufficient and nanogenerators have been recognized a suitable energy source in the last decade. The mechanical energy created by the daily activities of the human body is an accessible and natural energy source for nanogenerators. Fiber-structured functional materials contribute to the increase in energy efficiency due to their effective surface to volume ratio while providing the necessary compatibility and comfort for the movements in daily life with its flexibility and lightness. Among the potential solutions, electrospinning stands out as a promising technique that can meet these requirements, allowing for simple, versatile, and continuous fabrication. Herein, wearable electronics and their future potential, electrospinning, and its place in energy applications are overviewed. Moreover, piezoelectric, triboelectric, and hybrid nanogenerators fabricated or associated with electrospun fibrous materials are presented.

1. Introduction

As a result of the rapid developments in science and engineering in the 21st century, sensor networks have been developed rapidly and made the Internet of Things (IoT) applications an active part of our lives. Wearable electronics, in general, can be placed on clothes, accessories, or skin, enables people to constantly monitor their body movements and health, and receive feedback. These features make them indispensable future personal assistants fulfilling the needs of the people and an essential part of the IoT. Today, the limitations and challenges of this technology mostly stem from the need for a lightweight, flexible, small, and sustainable power supply for the sensors and electronic devices that built up wearable electronics. These requirements are still not well satisfied by the size and short life of the existing battery technologies. Nanogenerator technology, which collects various energy sources and converts them into electrical energy, was proposed as an alternative to battery technology and is ideally suited for these systems.[1]

Nanogenerators were first invented by Wang in 2006 and then several nanogenerators have been developed based on piezoelectric, triboelectric, and pyroelectric effects.[2,3] Among them, nanogenerators based on piezoelectric and triboelectric effects draw attention due to their simpler structure and the fact that human movements provide a good source of mechanical energy. Increasing the efficiency of energy conversion and obtaining higher power output from more compact devices is the focus of many studies. For this purpose, studies on material and system design are generally carried out. In terms of material design, micro/nanofiber materials fabricated by electrospinning contribute significantly to the performance of the devices since it allows the fabrication of fibers with a high surface to volume ratio and their alignment at the molecular level.[4] Moreover, electrospinning is a quite simple and convenient technique for mass production, and the resulting fibers respond to the flexibility requirements of wearable electronics devices.[5] Various polymers and polymer–ceramic composites have been processed by electrospinning due to ease of fabrication, being lightweight and cost-effective of the resulting fibrous material. For example, polyvinylidene fluoride (PVDF) and its copolymers are often used alone or in combination with functional materials.[6–9]

This study summarizes the trajectory of wearable electronic devices both in industry and in academia, the application of piezoelectric, triboelectric, hybrid sensors, and self-powered

T. A. Arica, Prof. M. M. Demir
Department of Materials Science and Engineering
İzmir Institute of Technology
İzmir 35433, Turkey
E-mail: mdemir@iyte.edu.tr

Dr. T. Isık
Department of Mineral Analysis and Technologies
General Directorate of Mineral Research and Exploration
Ankara 06520, Turkey

Dr. T. Guner
Centre Energie, Matériaux et Télécommunications
Institut National de la Recherche Scientifique (INRS)
1650 Lionel-Boulet Blvd, Varennes, Quebec J3X 1S2, Canada

Dr. N. Horzum
Department of Engineering Sciences
İzmir Katip Çelebi University
İzmir 35620, Turkey

The ORCID identification number(s) for the author(s) of this article can be found under https://doi.org/10.1002/mame.202100143

DOI: 10.1002/mame.202100143

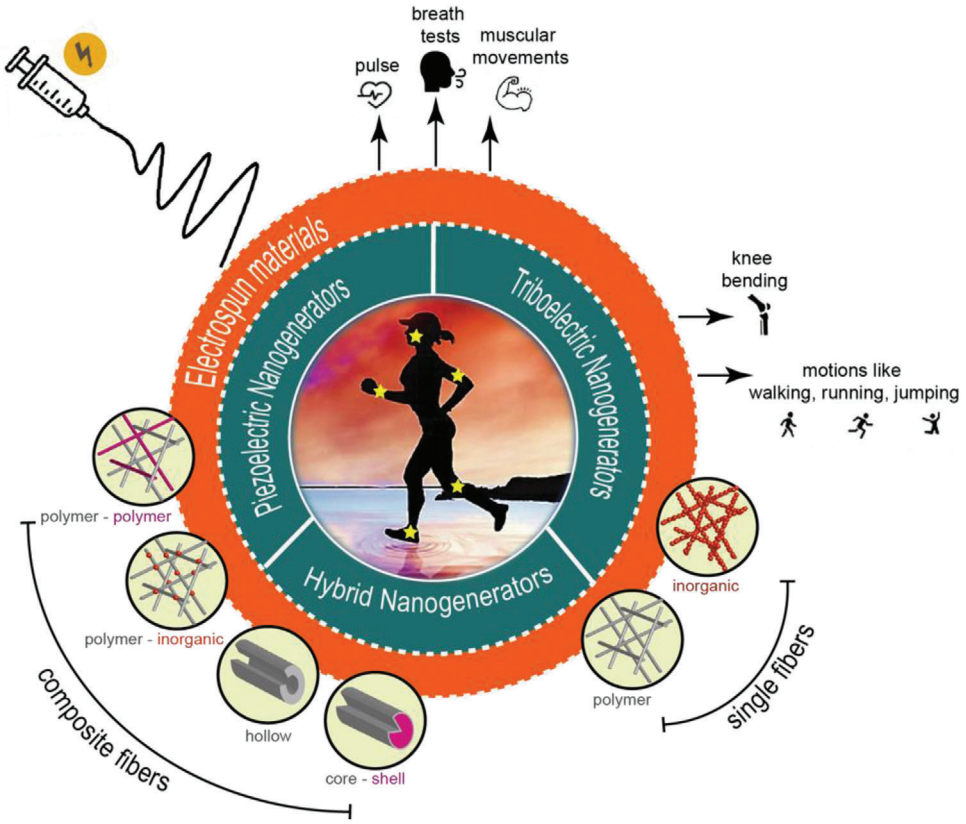

Figure 1. Electrospun fiber-based piezoelectric, triboelectric, hybrid nanogenerators.

nanogenerators associated with electrospun fibers (**Figure 1**). Piezoelectric and triboelectric effects are briefly explained and their production with selected functional materials and various electrospinning techniques are reviewed.

The scientific activities and popularity on wearable electronics can be traced by analyzing how publication records and citations vary in time (**Figure 2**). The keyword "Wearable Electronics" has been used to demonstrate a general trend in this field and some related subfield publications were also additionally refined by filtering "Electrospinning" and "Nanogenerator" keywords individually. Such a filtering can leave only the corresponding publication records and citations referring to electrospinning and nanogenerator within the context of wearable electronics, respectively.

Left panel of Figure 2 demonstrates that publications and citations related to wearable electronics have been started to increase dramatically after 2012. On the one hand, this increase may indicate that this field has already started to attract significant attention lately; and interest in this field will probably continue to rise in the next years since increment in both publication records and citations with respect to years is still far from saturation. On the other hand, electrospinning related wearable electronics publications records (middle top figure), start to saturate in recent years while citations (middle bottom figure), keep growing as similar to only "wearable electronics" case. Such an observation can indicate that of even though there is a strong interest in this field (based on the citation data), there are not many groups working on this field in order to reach more publications each year. Moreover, "Nanogenerator" related studies within the context of wearable electronics were also investigated. The increment in publication records and citations, right figures, follows a very similar trend which was observed already in "Wearable Electronics." This particular field has started to rise dramatically after 2014 and still keeps growing. Both "Wearable Electronics" and its "Nanogenerator" filtered dataset indicate a more dramatic rise in citations than reported publications. Such a difference may imply these fields even though they attract significant attention, are not producing sufficient publication outputs as similar to the electrospinning case. Therefore, it may be concluded that wearable electronics together with its electrospinning and nanogenerator subfields are new, open, and promising subjects today for researchers and even newcomers to these fields, which allows them to find numerous opportunities and challenges to overcome as part of their future studies.

2. Wearable Electronics

Trends in publication and citation data reflect the demand and interest that exist for wearable electronics, and among many possible advancements, wearable electrospun materials stand out as promising for the next decade. In general, wearable electronics is a popular and highly demanding field that has been attracting significant attention by both academia and industry in recent years. There are many types of market research providing an outlook for the expected possible growth of the corresponding market size for the future. For instance, a report "Wearable Electronics Market by Product and Geography—Forecast and

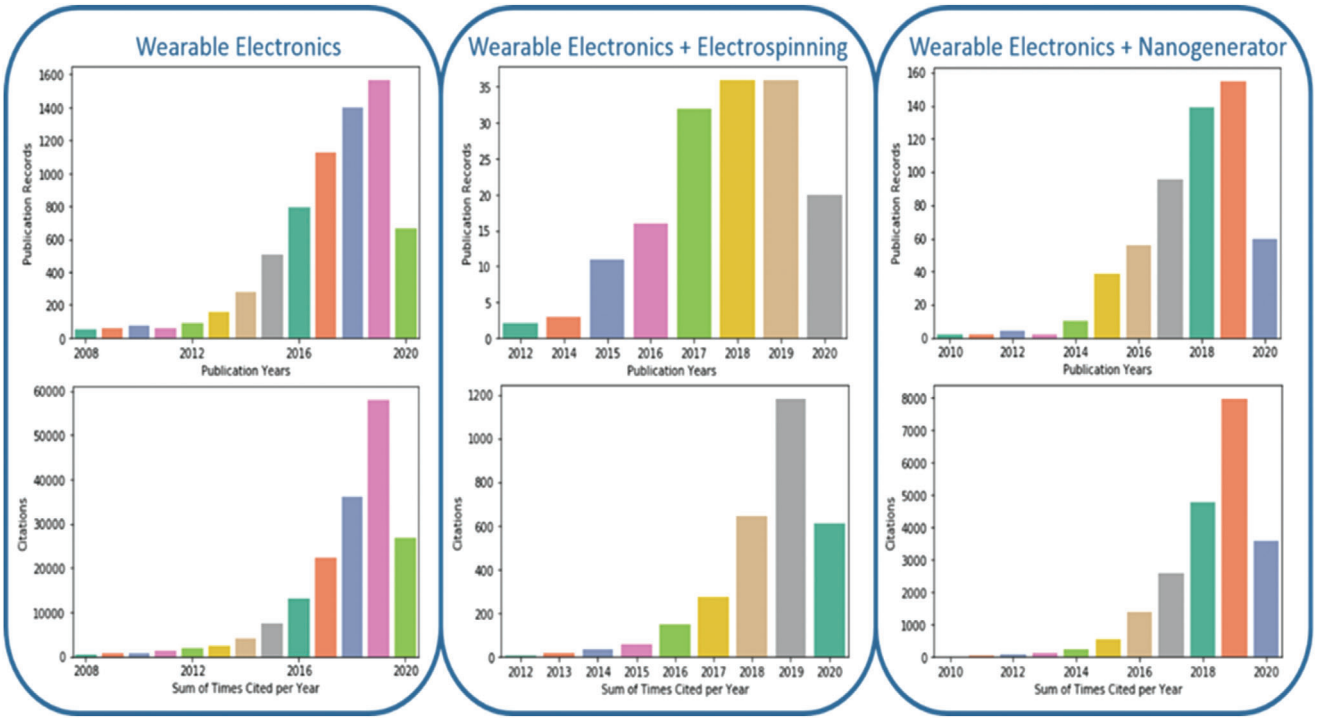

Figure 2. Statistical distribution of publication records and citations of "Wearable Electronics", "Wearable Electronics" + "Electrospinning" and "Wearable Electronics" + "Nanogenerator" keywords with respect to publication years and sum of times cited per year. All data was collected using WoS analytics.

Analysis 2020-2024" published in April 2020 forecasting a potential growth for the wearable electronics market by $41 billion between 2020 and 2024.[10] A previous report concerning the wearable electronic market growth between 2013 and 2020 estimated a $25 billion market size, which is almost half of the estimated one for 2020–2024 above.[11] Such a rapid market growth reveals and hints about its huge potential for the near future. Apart from the total market growth, market share distribution of several wearable electronics-related products such as basic watches, smartwatches, wristband, clothing, ear ware, and other can be tracked in time to understand the direction of trending. For example, **Figure 3** demonstrates that wristband is losing its market share continuously from 2018 to 2021 by dropping from 37.86% to 23.88%. On the other hand, clothing showing a huge leap from 2.60% to 8.19%, and smartwatches increase their share from 24.48% to 30.97%. In this sense, more products will appear, and more sales are anticipated to be made in smartwatches and clothing related products in the future.[12]

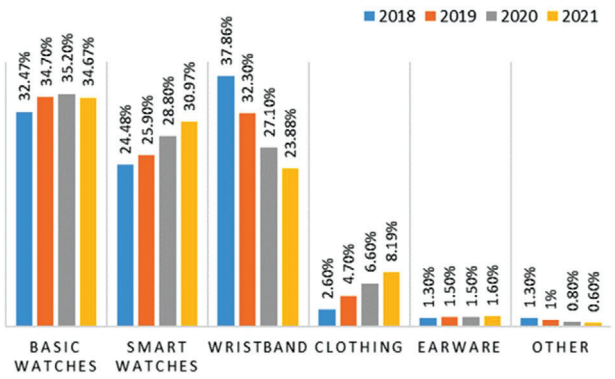

Figure 3. Excepted market share distribution of different wearable electronics products between 2018 and 2021. Reproduced with permission.[12] Copyright 2020, Elsevier Ltd.

Wearable electronics have a broad range of application areas from smart clothes to health monitoring devices, from displaying technologies to sensors, etc.[13–19] Basically, wearable electronics favor flexible and stretchable electronics to be embedded in a biocompatible and soft matrix to operate over the skin while allowing users to perform any motion and movement like bending, jumping, running, or involving any human joint rotation, vibration, etc. without any restriction, which can suppress those activities resulting in an inefficient use. Wearable hybrid electronics,[16] which combines biocompatible, flexible, and soft materials with miniaturized devices that can be attached to corresponding materials to generate outputs like sensors, monitoring devices, batteries, etc., can be given as an example. However, most of the existing products today contain rigid supports, which is the inevitable outcome of the required stable conductivity since it is still a challenge to satisfy it with flexible/stretchable material systems. This trade-off between having sustainable conductivity and being stretchable or flexible is one of the major issues that has been tackling as a part of ongoing research in this field.[20–26]

On the other hand, since wearable electronics require flexibility, softness, light weightiness, and small in size device

architectures, such conditions then automatically induce the necessity of the design of flexible, lightweight, and small sustainable power supplies.[27–29] These units are responsible for supplying power for the devices attached to the wearable electronics. There are various methods that aim to generate electricity through converting mechanical, solar, thermal, and biofuel energies.[30–37] However, even these strategies can provide high conversion efficiencies, they are mostly not eligible due to their rigid structure that not allowing them to be reduced in size or due to their lack of operation while under stretching and bending. Also, their performance depends on external factors excessively like sunlight and temperature. Apart from this well-known energy harvesting and energy conversion strategies, since wearable electronics are mainly designed to be worn by humans, it becomes possible to design self-powered power supply units that can generate power by converting biomechanical action or body temperature into electricity.[27,38–40]

3. Electrospinning

Nanofibers have been attracting considerable attention in recent years due to their remarkable properties. Among various fiber fabrication techniques such as melt-blowing,[41] template synthesis,[42] self-assembly,[43,44] and phase separation,[45] electrospinning is the most preferred technique due to its tailorable properties, efficiency, and cost-effectiveness.[46] The ability to produce 2D nanofibrous and 3D macrostructures with exceptionally long in length and uniform in diameter makes electrospinning one of the facile and very simple fiber fabrication technique.[47–49] Compared to the conventional fiber fabrication techniques, electrospinning permits the fabrication of nanofibers with enhanced surface area, controllable porosity, extremely long length, alignment on the molecular level, and lightweight nature which are needed for various fields[50] such as tissue engineering,[51,52] filtration,[53–55] functional materials in industrial applications,[56–59] sensors,[60–62] and energy harvesting applications.[63,64]

The adventure of electrospinning dates back to 1934 with the revealing of the electrostatic spinning patent, which describes the production of polymer filaments using electrostatic repulsions of surface charges.[65] However, the investigations about the effect of electrostatic interactions on solutions started in the 1960s that William Gilbert observed the deformation of the fluid droplet from spherical to cone under the electrical field.[66] Then, Geffrey Taylor reported the existence of "Taylor cone" in fluid droplets that this cone has a conical angle of 49.3° and forms under the effect of the electrical field.[67] Also, the author investigated the Rayleigh and bending instabilities, which improve the mechanisms behind the electrospinning technique. Afterward, in the early 1990s, the Reneker group has interested to fabricate thin fibers from a wide range of polymers and the technique has started to be called electrospinning. The group investigated the bending instability of charged jets and supported their findings with theoretical results.[68] On the other hand, different models have been described by Rutledge and co-workers that whipping instability is the main process during the electrospinning and electrostatic interactions between electrical field and surface charges.[69]

3.1. Basic Principles and Different Configurations of Electrospinning

The electrospinning set-up mainly consists of four components, which are a high voltage supply (DC or AC current), a spinneret or a conductive needle, a syringe pump, and a grounded collector (**Figure 4**). The polymer solution or melt feeds the spinneret with the help of a syringe pump and a high voltage (from 1 to 30 kV) is applied to the conductive needle. The polymer jet becomes highly charged and is exposed to electrostatic repulsion between surface charges and Coulombic force by an external electrical field.[50] The repulsion between charges on polymer solution tries to beat the surface tension and the droplet starts to be deformed by forming a Taylor cone. After a while, the electrical field exceeds the critical value by overcoming the fluid surface tension, and the polymer solution generates fluid jets through the electrical field. During the transportation of fluid jets under the electrical field, the solvent is evaporated from the jet and dry nanofibers are collected on a grounded collector.[70]

Besides the extremely simple set-up of electrospinning, the mechanism behind the fiber fabrication is rather complicated. The technique is based on the electrostatic interactions where electrical drawing force is directly applied to the viscoelastic fluid and elongation of polymer jet generates continuous fibers[50] that distinguish this technique from other fiber fabrication methods. Initiation of the jet, whipping instability, and fiber deposition take place during the process. Whilst the conical shape forms, the polymer jet becomes sharp and is emitted from the tip of the needle. The electrical field accelerates and thins the charged jet and this part of the process is called jet initiation. Afterwards, jet instabilities (whipping instability) have been observed because of the charges on the jet and different movements could be observed such as bending, looping, spiraling, and winding. Until 1999, the formation mechanism behind the thin fibers has been ascribed to a splitting of the charged jet during the electrospinning.[49] However, the bending and whipping instability of the charged jet is associated with the main reason for thin fibers that the jet forms in a straight form at the beginning and then became unstable by bending or whipping processes.[71] In the final stage, the solvent evaporates, and the jet gets dry by depositing on the grounded collector.[46]

Electrospinning provides an opportunity to tailor the final structure and morphology of fibers by modifying the set-up or parameters in different ways. There are many processing parameters, which affect the diameter and morphology of electrospun fibers. The solution parameters such as type and molecular weight of polymer; solution concentration, viscosity, surface tension, and electrical conductivity have substantial effects on the resulting morphology of fibers. For example, at low polymer solution concentration, electrospraying takes place instead of electrospinning because of the low entanglement of polymers or at very high solution concentration, high viscoelasticity of solution inhibits the formation of fibers.[70,72] Applied voltage, flow rate, and tip-to-collector distance are called operational parameters and they are effective for the fiber morphology. Because tip-to-collector distance directly affects the electrical field, the final diameter of fibers changes accordingly with this parameter. Moreover, the polymer jet needs sufficient time for the evaporation of the solvent during transportation from tip-to-needle.

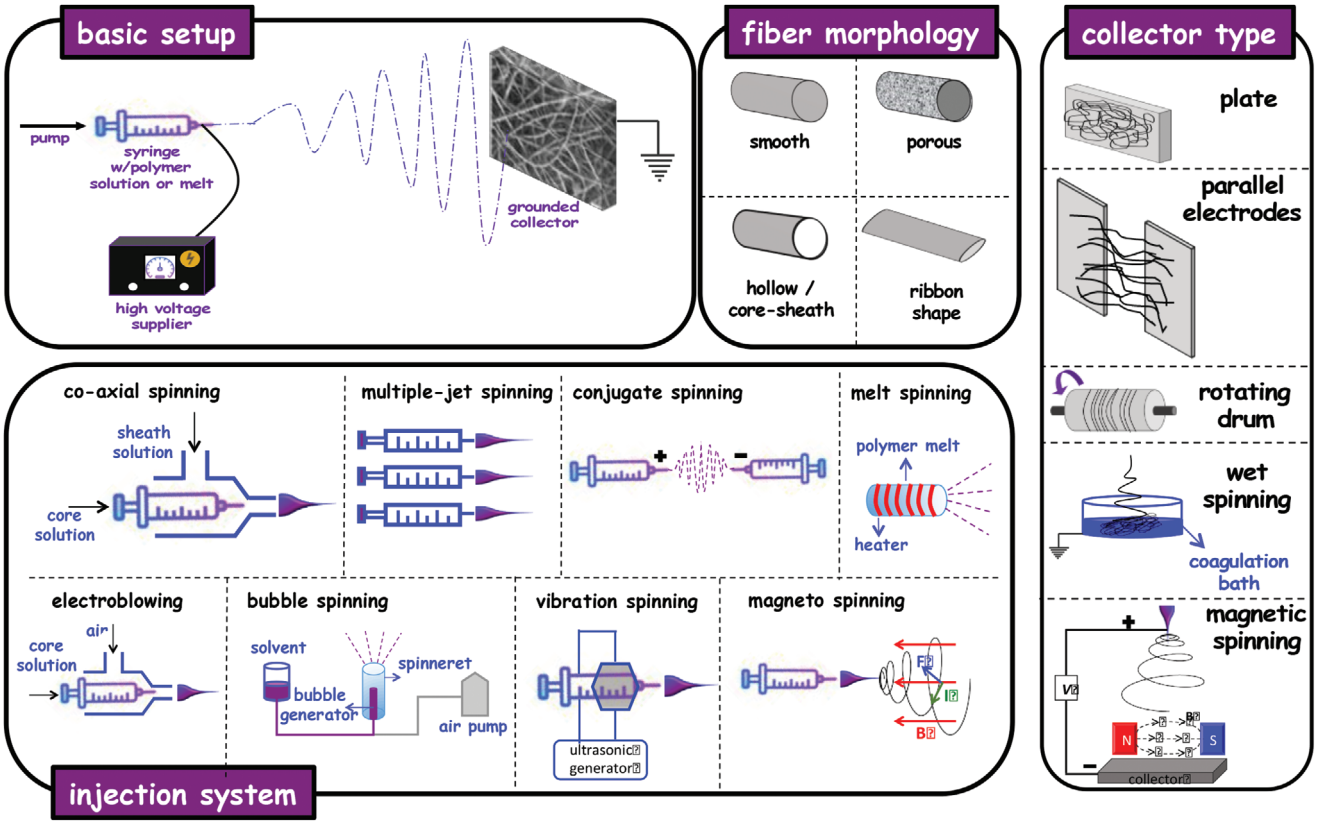

Figure 4. Basic electrospinning setup and possible fiber morphology with different injection system and collector types.

Thus, this distance is very important for the appropriate dryness of fibers.[73–75] To overcome the surface tension on the polymer droplet, the applied voltage should provide an adequate electrical field to the solution. As the applied potential difference increase, the diameter of fibers decreases because of the improved stretching forces.[76,77] Besides, the fabrication rate of fibers depends on the flow rate of the polymer solution such that a higher flow rate results in coarse fibers.[78] Apart from these parameters, environmental parameters such as temperature and humidity have remarkable effect on morphology of the fiber. Because temperature may affect the crystallization of polymer and result in the porous structure, whilst humidity may affect the final porosity of fibers because of the phase separation of solvent and water in the air.[79] Also, conventional electrospinning systems have single needles, which feed the solution at a slow rate. Thus, multiple needle systems have been used to enhance the fabrication rate of fibers. Apart from the single needle systems, a multineedle or needless electrospinning set-up has been developed to enable the mass production of fibers.[80]

The way in which you deposit the fibers on the grounded collector is an important parameter that the orientation of fibers can be achieved by changing the layout or shape of the collector.[81] In general, the fibers are randomly deposited on the collector without any specific structure. However, aligned or core-sheath structured nanofibers might be desired for specific applications. Thus, there are numerous ways to change the fiber deposition on the collector (Figure 4). Deposition of uniformly aligned fibers can be achieved by using a high-speed rotating drum[82] or parallel electrodes[83] as a collector that the tensile strength of fibers can be improved in this structure. Wet spinning is a relatively complex process when compared with other spinning techniques. The setup is similar to the basic vertical-electrospinning set up apart from the collector part that electrospun fibers are collected on a grounded or negatively charged liquid bath, such as water, and the resulting fibers are precipitated in that liquid.[84] As an example, it is difficult to process cellulose in its melt form however, it has been found that cellulose can be dissolved in hydrophilic ionic liquids. Although the main drawback of using ionic liquids is their cost, using the wet spinning technique can solve this problem that more than 99.5% of the solvent can be recovered after the process.[85,86] Magnetic electrospinning is another facile approach for the fabrication of well-aligned fibers that polymer solution is magnetized by the addition of small amount of magnetic nanoparticles and the fibers are fabricated in the presence of a magnetic field, which is generated by two parallel magnets.[87,88]

Electrospinning can be carried out by changing the injection system in different ways (Figure 4). Reducing the distance between the tip of the spinneret and collector in the microscale is called near-field electrospinning (NFES). In this way, the deposition of fibers on the collector is controlled and Lin et al. fabricated fibers with diameters ranging from 50 to 500 nm.[89] NFES has outstanding features when compared with conventional electrospinning. For instance, the positioning of individual fibers is possible with high precision and control of fiber morphology is possible when single fibers are desired for photonic applications.[90] In addition to the NFES, hydrodynamic writing is another fiber

fabrication technology that lower electrical potential can be used for the process and this technique has been employed using alternating mode instead of stable jet mode.[91] The combination of two axial capillaries in a syringe system can be used for the fabrication of core-sheath structured or hollow nanofibers.[92,93] Different types of solutions feed the outer and inner needles and high voltage drives out the combined coaxial jet. The coaxial jet may have a composite structure with two different polymers, a polymer shell with particles inside or hollow structure.[94,95] Using a temporary material as the core and removing that material with a post-process can achieve the fabrication of hollow fibers. For instance, oil is often used as a core because it can be easily removed and hollow fibers with an empty core can be procured.[95,96] Electroblowing has a similar setup with the co-axial system but the outer syringe creates airflow around the spinneret and the additional stretching force provided by the gas jet leads to the formation of thinner fibers.[97] For the mass production of fibers in industrial applications, such as the textile industry, increasing the number of needles on spinneret is the simplest approach that is referred to as multiple-jet spinning. The polymer solution is pumped through the spinneret with multiple needles and high voltage is needed for the continuous spinning. In this system, different solutions can be pumped for different needles by using more than one syringe pump and blended fibers. However, the cleaning of clogged needles is a problem for these setups that unstable electrical fields may result in the variation of final fiber morphology.[80] Fibers with high mass production rates can also be obtained by melt spinning technique that a polymer melt is taken into a syringe, which is coated with a heater thereby the polymer melt is prevented from coagulation. One of the simplest techniques for the mass production of continuous fibers is bubble electrospinning that needless electrospinning setup has a bubble generator as shown in Figure 4. The aerated polymer solution forms bubbles in the absence of an electrical field and subsequently applied electrical field induces the charges on the surface of the bubble. The applied electrical field and coupling of surface charge result in a tangential stress on the bubbles by deforming them into a jet.[98] Conjugate electrospinning involves two high voltage supplies with opposite polarity with two different spinneret systems. This setup enables the simultaneous collection of two different polymers on the same collector that results in composite fibers with varied morphology. Another composite fiber fabrication technique is emulsion electrospinning that feeds polymer solution consisting of two or more polymers, which are insoluble with each other. The resulting fibers may not have continuous core–shell morphology, but different phases of polymers can be represented in the same structure. This technique is beneficial for drug-delivery applications in tissue engineering applications.[84] Vibration technology has been applied to polymer solutions to reduce the viscosity, which leads to producing fine fibers with less voltage. Vibration force weakens the Van der Waals force of macromolecules and entanglement of fibers is relaxed that results in a reduction in viscosity.[99,100] The instability during the electrospinning destroys the molecular orientation and mechanical properties of fibers. Magneto-electrospinning controls the instability during the process. When a magnetic field is applied, the current on the jet produces a centripetal force, which shrinks the radius of whipping jet and, the stability of jet is improved.[99,101]

3.2. Electrospinning in Energy Harvesting Applications

Harvesting energy from the surrounding environment, such as mechanical loads or human body movements, and conversion of this energy to electricity for wearable electronic devices receive remarkable attention. Thus, the development of micro- and nanogenerators has been encouraged to harvest the energy mechanically or piezoelectrically and conversion of this energy to electricity for self-powered devices.[102–104]

Piezoelectric materials, which have noncentrosymmetric crystal structures, are able to generate electrical potential as a result of the lattice distortion and polarization changes with the application of stress.[105] Therefore, the utilization of piezoelectric electrospun fibers has been gaining attention due to their excellent flexibility and strength.[106] PVDF is a piezoelectric polymer with a semicrystalline structure and has a spontaneous polarization feature due to the electrostatic β-phase. It is a widely used polymer in piezoelectric nanogenerators (PENGs) and electrospinning leads to the transition of other phases to the electroactive phase by mechanical stretching or poling.[107] When compared with inorganic piezoelectric materials, such as lead zirconate titanate (PZT), electrospun PVDF have a greater potential in wearable applications due to its flexible, easily processable, and lightweight nature.[105] Furthermore, PVDF fibers can be used in the fabrication of triboelectric nanogenerators (TENGs) that polydimethylsiloxane (PDMS) coated PVDF fibers have improved mechanical robustness and can be used in wearable TENGs.[108] Therefore, electrospun fibers have been shown to be alternative materials for energy harvesting applications, particularly in wearable electronics.

4. Nanogenerators with Electrospun Based Materials

The fabrication of small, flexible, and low energy-consuming personal electronic devices in a practical way without the need for batteries is vital for modern life. The consumption of power for such devices usually lies between micro and milliwatts.[109] Therefore, they need to be powered by a sustainable and self-powered energy source that collects energy from the environment. Nanogenerators (NGs) are small and lightweight devices that convert various types of energy such as mechanical (i.e., pressure, vibration, bending, stretching) and thermal into electricity even at a low frequency using a physical model of Maxwell's displacement current as a driving force.[110] These features of nanogenerators make them the most suitable and powerful candidate for making self-powered sensors and powering wearable electronic devices. In recent years, NGs have been extensively studied by focusing on material, device design, and function. Maximization of efficiency in energy conversion largely depends on the material design and structure, and this goal is achieved by micro/nanostructured materials with high specific surface area. Electrospun derived nanostructures including nanofibers and nanoparticles can be readily fabricated in a single step, or with simple post-processes like grinding or heating at a low cost. In this review, piezoelectric, triboelectric, and piezoelectric-triboelectric hybrid NGs prepared by electrospinning from various material combinations were highlighted in terms of material design, function, and performance of the devices.

4.1. Piezoelectric NGs

Piezoelectricity refers to a material's ability to generate an electrical charge when subjected to mechanical deformation in an appropriate direction. Mechanical deformation causes charge center displacement, which results in electrical polarization of the noncentrosymmetric unit cell. An electrical potential can be measured as a result of applied mechanical deformation if electrodes are placed on the surface of the crystal. This phenomenon is of great interest in the field of self-powered sensors and nanogenerator technologies. Piezoelectric NGs (PENGs) transform mechanical energy into electricity through the external circuit which collects, and transfers charge induced by mechanical stress in nanostructured piezoelectric materials. Besides being used to collect energy from various sources such as body movement, sounds, and wind; self-powered sensor applications of PENGs have also been extensively studied.[9,111–113]

4.1.1. Piezoelectric Materials Used in NGs

Piezoelectric effect can be observed in both organic and inorganic materials, which have no symmetry center at their crystalline state. The widely studied piezoelectric ceramic materials such as barium titanate ($BaTiO_3$), PZT, barium zirconate-titanate/barium calcium-titanate ($[(BaZr_{0.2}Ti_{0.80})O_3]_{1-x}$-$[(Ba_{0.70}Ca_{0.30})TiO_3]_x$ ($x = 0.10, 0.15, 0.20$), BZT-BCT), potassium sodium niobate ((K, Na)NbO_3, KNN) are known for their high piezoelectric coefficient, but they are hard and lack of the flexibility that restricts their use in wearable electronic devices. On the other hand, piezoelectric polymers have advantage over ceramics in terms of flexibility, stretchability, and being lightweight.

PVDF and its copolymers such as poly(vinylidene fluoride-trifluoroethylene) (P(VDF-TrFE)) and poly(vinylidene fluoride)-*co*-hexafluoropropylene (P(VDF-HFP)) are the most commonly employed piezoelectric polymers. In addition, they are biocompatible, chemically stable, and easily synthesized. PVDF exhibits five different semi-crystalline polymorphs with different chain conformation which are α (TGTG'), β (TTTT), γ (T_3GT_3G'), δ (polarized α), and ϵ phases. The stable phase among them is the nonpolar α-phase. The polar crystal structure β-phase of PVDF shows the highest piezoelectricity due to the electric dipole moment developed by the off-symmetry distribution of negatively charged fluoride ions.[114] Various strategies have been applied to achieve a high amount of β-phase such as mechanical stretching, strong electric field exposure, additive addition, annealing, and high-speed cooling during melt crystallization. Additionally, the 1D nanostructured-PVDF fibers have higher efficiency in the conversion of piezoelectric energy compared to that of PVDF film.[115] Electrospinning is a single-step process to obtain β-phase rich content PVDF fibers by combining electrical polarization and mechanical stretching.[116] Therefore, electrospun PVDF fiber membranes are widely used for the fabrication of PENGs.[117–119]

4.1.2. Electrospun Fiber-Based PENGs

The most widely used piezoelectric polymer, PVDF, processed by electrospinning still contains the nonpolar α-phase. To increase β-phase, mechanical stretching and electrical polarization can be applied as postprocessing.[113,117,120] Ma et al. peeled off P(VDF-TrFE) as-spun fibers from aluminum foil and mechanically stretched them at 2 mm s^{-1}.[113] The average output voltage of majority of (80%) aligned fibers is 0.08496 V, around 266% of their randomly distributed equivalents, and their mechanical strength is better. In addition, the aligned fibers are twisted into fiber bundles and then woven into an outfit that can sense body motion (**Figure 5**a–f). Liu et al. prepared a polarized electrospun PVDF membrane to make PENG that can be used as a self-powered respiration sensor. The output voltage and the short-circuit current of device were 1.5 V and 0.400 µA, respectively.[117] Also, using a high-speed rotating drum collector instead of a flat collector provides additional mechanical stretching on the fibers.[6,111] Generally, highly aligned, and vast amounts of β-phase PVDF fibers are obtained at rotational speeds nearly higher than 1000 rpm. You et al. fabricated aligned P(VDF-TrFE) nanofibers with 76% β-phase content by using parallel electrodes and a rotating drum collector. P(VDF-TrFE) nanofibers based nanogenerator exhibit 12 V output voltage and 0.150 µA short circuit current.[121] To further improve nucleation and stabilization of the β-phase, researchers have presented studies on the doping of fibers with inorganic nanofillers.[111,112,122–126] Besides, the addition of nanofillers may enhance the mechanical and thermal properties of the polymers.[9,111,124,127,128] Ghosh et al. fabricated platinum (Pt) nanoparticle doped PVDF nanofibers with a 75% degree of fiber alignment by using a high-speed rotating drum (2000 rpm). The mechanical properties of the nanofibers improved as the degree of crystallinity increased. Wearable NG structure was formed by placing fibers between the flexible conductive fabrics. Pt-PVDF nanofibers show five times higher piezoelectricity than that of neat PVDF nanofibers.[111] Khalifa et al. added graphitic-carbon nitride (g-C_3N_4) nanosheets to PVDF fibers to provide high β-phase content. Also, the g-C_3N_4 nanosheet has a negatively charged surface that increases the spinnability and improves the piezoelectric properties of PVDF.[127] Alam et al. used titanium dioxide (TiO_2) nanoparticles for the enhancement of β-phase and mechanical property of PVDF fibers.[9] Jin et al. developed a bending sensor as a candidate for the self-powered respiratory monitoring device (Figure 5g–i).[125] Silver (Ag) nanoparticles doped PVDF solution was electrospun with a rotating drum at 2000 rpm for the obtainment of highly aligned and β-phase rich content fiber. Adhikary et al. fabricated Eu^{3+} doped P(VDF-HFP)/graphene fiber by electrospinning for ultrasensitive PENG. Doping Eu^{3+} and graphene sheets into P(VDF-HFP) nanofibers provides the full conversion to β-phase and the increase of the degree of crystallinity. Obtained PENG can sense external pressure ~23 Pa with a high degree of acoustic sensitivity (11 V Pa^{-1}) meaning that this mechanism may be used to identify human voices.[126]

Despite the various advantage of piezoelectric polymers, their piezoelectric coefficient significantly lower than that of piezoelectric ceramics. To address this drawback, the fabrication of polymer-ceramic nanocomposite has been proposed as a new type of piezoelectric material for NGs.[8,112,122,123,127,129–134] The synthesis of these two materials in the form of fiber or film structure can result in a more functional material. Various types of piezoelectric nanofillers have been incorporated into the PVDF fibers to improve their piezoelectricity. PZT is the most favorable piezoelectric ceramic material due to its high piezoelectric

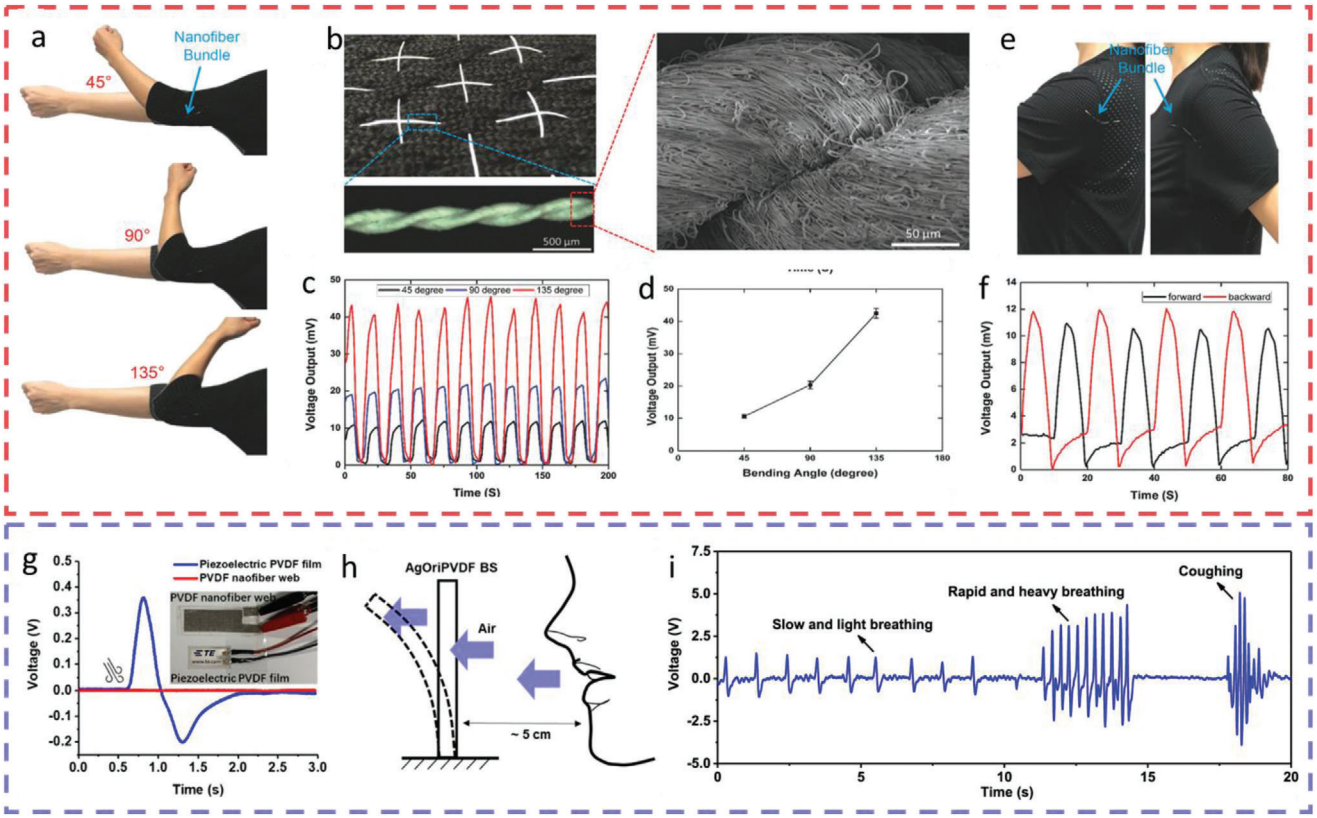

Figure 5. Applications of electrospun fibers. a) Twisted electrospun P(VDF-TrFE) fiber bundle woven into the outfit. b) Monitoring different bending angles of elbow movement using twisted P(VDF-TrFE) fiber bundle. c) Corresponding voltage outputs and d) their average values. e) Two directions of the arm swing and f) their corresponding voltage outputs. Reproduced with permission.[113] Copyright 2018, John Wiley and Sons; g) Comparison of response to the expired air between the commercial piezoelectric PVDF film and the electrospun PVDF nanofiber. h) Schematic of the respiration measurement setup. i) Various breathing patterns detected. Reproduced with permission.[125] Copyright 2020, American Chemical Society.

coefficient ($d_{33} \approx 200$–750 pC N^{-1}) but it is harmful to humans and is not environmentally friendly. Therefore, in most studies, lead-free $BaTiO_3$, zinc oxide (ZnO), BZT-BCT, KNN, zinc sulfide (ZnS) was preferred instead of PZT.[112,129–132,135] In earlier studies, different piezoelectric nanocrystals have been used together to enhance the electrical output of piezoelectric NGs. Sabry and Hussein added ZnO nanorods and $BaTiO_3$ nanospheres fillers to the PVDF fiber matrix, and a 12 V electrical output was observed under a force of 1.5 N.[131] Mostly, the piezoelectric nanofillers added also induce the PVDF β-phase that contributes to the improvement of the electrical performance of the material. Alam et al. doped PVDF nanofibers with ZnO-containing paper ash and enhancement of β-phase content was observed. The fabricated NG serves as a wind flow energy harvester and active sensor and it provides a high output of 4.8 V under 145 Pa exerted wind flow.[112] Parangusan et al. reported the fabrication and piezoelectricity of P(VDF-HFP) matrix Co-doped ZnO reinforced composite nanofibers by electrospinning.[122] The undoped ZnO (1 wt%) and Co-doped ZnO (0.5, 1.0, and 2.0 wt%) nanoparticles were dispersed into the solution of P(VDF-HFP) in a mixture of DMF and acetone. Structural characterization conducted with XRD and FTIR studies show that the increase of Co-doped ZnO nanofiller concentration in the P(VDF-HFP) matrix results in increased piezoelectric polar β-phase. P(VDF-HFP)/Co-ZnO (2 wt%) nanofibers have higher β-phase content than the neat P(VDF-HFP) sample. The dielectric constants of the P(VDF-HFP) and P(VDF-HFP)/Co-doped ZnO (2 wt%) were found to be approximately 8 and 38, respectively. The piezoelectric output voltage for 2 wt% Co-ZnO/P(VDF-HFP) nanofibers was as high as 2.8 V compared to P(VDF-HFP) nanofibers (≈120 mV). However, the electroactive β-phase content does not always increase with an increasing the amount of additives, usually, it has a threshold value.[127] Some studies have been shown that the β-phase content decreases as the amount of filler increases, and yet the device voltage output increases.[129] Bairagi and Ali developed electrospun PVDF fibers containing KNN nanorods (≈8.5 aspect ratio) in various percentages (0%, 1%, 3%, and 5%). A decrease of β-phase content has been observed with an increase in the percentage of KNN nanorods. β-phase content for pure PVDF, 1%, 3%, and 5% KNN nanorods were noted as 97%, 89%, 78%, and 84%, respectively. The fabricated PENG using 3% KNN nanorods showed the highest values with 17.5 V output voltage and 0.522 μA output current.[129] Morphology of the inorganic filler also influences the amount of β-phase of PVDF. Li et al. discussed the effect of ZnO nanorods and nanoparticles on the β-phase of PVDF and piezoelectric properties of electrospun composite material. The electroactive β-phase content of ZnO nanorods/PVDF was calculated as 90.7% and that of the ZnO nanoparticles/PVDF

was 87.5%. The output voltage and short circuit current of ZnO nanorods/PVDF and ZnO nanoparticles/PVDF were found as 85 V, 2.2 μA and 60 V, 1.7 μA, respectively. Synergistic effect of the both piezoelectric ZnO nanorods and increased β-phase of PVDF result in higher-performance piezoelectric.[123]

Electrospun polymer fiber matrix-based piezoelectric nanocomposites generally synthesized by dispersion of inorganic nanoparticles into the polymer matrix volume. However, this can cause the degradation of flexibility and mechanical properties due to the agglomeration of the nanoparticles. To overcome this problem, alternative ways of preparing materials are presented. Kim et al. reported the growth of ZnO nanorods on the surface of PVDF fiber by using a low-temperature hydrothermal method to improve piezoelectric response without losing breathability and flexibility.[133,136,137] The open-circuit voltage can be increased up to 2.3 times by growing the ZnO nanorod on the PVDF fiber using this method. Guan et al. prepared polydopamine modified $BaTiO_3$ nanoparticles and attached them onto the surface of P(VDF-TrFE) electrospun fibers (**Figure 6**a–e).[132] The hierarchically structured fiber-based PENG exhibited significantly improved output of 6 V and 1.5 μA as compared to PENG with pure P(VDF-TrFE) membrane that showed 1.25 V and 0.6 μA. In addition, up to 40% higher output voltage was obtained compared to composite membranes containing nanoparticles dispersed in nanofibers. To show a wearable application of the device, PENG is integrated into the insole of the shoe (Figure 6f–h).

In addition to the PVDF, poly (L-lactic acid) (PLLA) is also preferred for its shear-piezoelectric behavior in the fabrication of piezoelectric devices. PLLA has no intrinsic polarization; however, a slight change in the position of the molecular group C=O under the applied electric field by electrospinning reveals its piezoelectricity.[138] Sultana et al. developed high sensitivity (22 V N^{-1}) piezoelectric bio e-skin with a detection limit of 18 Pa based on the PLLA nanofiber membrane.[139] It has been shown that the device produced can be used to monitor human physiological signals such as voice recognition and wrist pulse (Figure 6i,j).

Electrospinning is a cost-effective and simple process to fabricate not only polymeric nanofibers but also inorganic nanostructures. It allows to obtain flexible, oriented, and high piezoelectric coefficient nanofibrous ceramic membranes, nanowires, and nanoparticles.[130,140–143] Liu et al. prepared P(VDF-TrFE) matrix and lead-free BZT-BCT (620 pC N^{-1}) nanoparticle composite nanofiber for the fabrication of PENG.[130] BZT-BCT nanoparticles were synthesized by electrospinning, calcination, and grinding steps as shown in Figure 6k,l. The amount of nanoparticle doping ranging from 0 to 50 wt% was studied and characterized by XRD and SEM. The nanogenerator prepared from composition with 40 wt% nanoparticles doped P(VDF-TrFE) fiber exhibit better performance among other compositions. The wearable application of the nanogenerator was shown with a device containing 40% BZT-BCT by weight and was attached to the finger, wrist, and elbow joint of the human (Figure 6m–o). Liu et al. synthesized $0.93(Na_{0.5}Bi_{0.5})TiO_3$–$0.07BaTiO_3$ (NBT-0.07BT) nanofibers by sol-gel based electrospinning.[143] As-spun fibers annealed at 750 °C for 2 h in air. For the fabrication of PENG, nanofibers were transferred onto the flexible electrode and polydimethylsiloxane (PDMS) coated on the fiber/electrode structure as a matrix material. The output voltage of PENG was ≈30 V under 1 MΩ resistance and the obtained average power was 1.5 μW.

The flexibility in use of the electrospinning setup is perfectly suited for fabricating textile yarns. Instead of integrating sensors and electronics into clothing or skin, providing functionality to textile fibers can give a different point of view to smart textile products. Electrospun piezoelectric fibers are convenient for functional smart textile yarns.[144–146] Yang et al. fabricated plied yarns from electrospun P(VDF-TrFE) nanofibers.[144] Piezoelectric yarns were subjected to post-processing (i.e., thermal annealing and stretching) to investigate their mechanical and material properties. Also, the fabrication of continually twisted yarns was made by using continuous electrospinning apparatus and woven piezoelectric fabrics thereof were shown (**Figure 7**a–f). The electrical and mechanical properties of yarns were enhanced due to the increment of crystallinity in the PVDF semicrystalline phase as a result of applied postprocessing. The output voltage of annealed fabric was 4.5-fold higher than that of as-made fabric. Gao et al. fabricated piezoelectric yarn by wrapping PVDF fiber around conductive filament with a customized electrospinning setup and then coating with PVDF film (Figure 7g–i).[145] The coating of PVDF nanofibers with PVDF film enhanced the interfacial property between the nanofiber layer and conductive filament. The resulting yarn generated an average peak voltage of 0.52 V, a peak current of 0.01876 μA, and a power density of 5.54 μW cm^{-3} under a cyclic compression of 0.02 MPa at 1.85 Hz, that is considerably higher than the energy output of yarn consisting of just the PVDF nanofibers layer. The performance of piezoelectric yarn was maintained after 50 000 cycles of compression. Ji et al. synthesized piezoelectric nanofibers from the BNT-ST ceramic powder doped P(VDF-TrFE) precursor solution and then core-shell piezoelectric yarns were fabricated by wrapping nanofibers around a conductive thread.[146] The outer electrode layer of the PENG incorporated by braiding of conductive thread with core-shell piezoelectric yarns. Obtained structure directly attached to the fabric (i.e., glove, guard, and shoe insole). The output voltages were studied during bending tests as a function of total length, effective area, sewing range of piezoelectric threads, and pressure.

Besides the conventional solution electrospinning, melt and NFES techniques are used to manufacture piezoelectric fibers. Melt electrospinning allows the production of low-porosity fibers of controlled diameter. However, molecular dipoles in fibers are randomly oriented because of the low applied voltage in melt-spinning, and therefore additional drawing and poling processes are required for the alignment to obtain a functional piezoelectric material (Figure 7j).[147] Steinmann et al. reported the crystallization and phase transitions in melt-spun PVDF fibers to optimize the formation of the β-phase for the piezoelectric effect in fibers. PVDF melt-spun fibers were processed by draw-winding, where the mechanical stress occurs, hence responsible for the formation of β-phase.[148]

NFES is a newly developed technique that stands out with its controllable deposition at low voltage.[149] Direct-writing and patterning of PVDF and its copolymer by using NFES were presented in recent studies.[150–155] Lee et al. presented a self-powered sound-sensing element from nano/micro PVDF fibers via NFES. The element placed on the throat can be distinguished from cough, swallowing, head tremors, and head-shaking

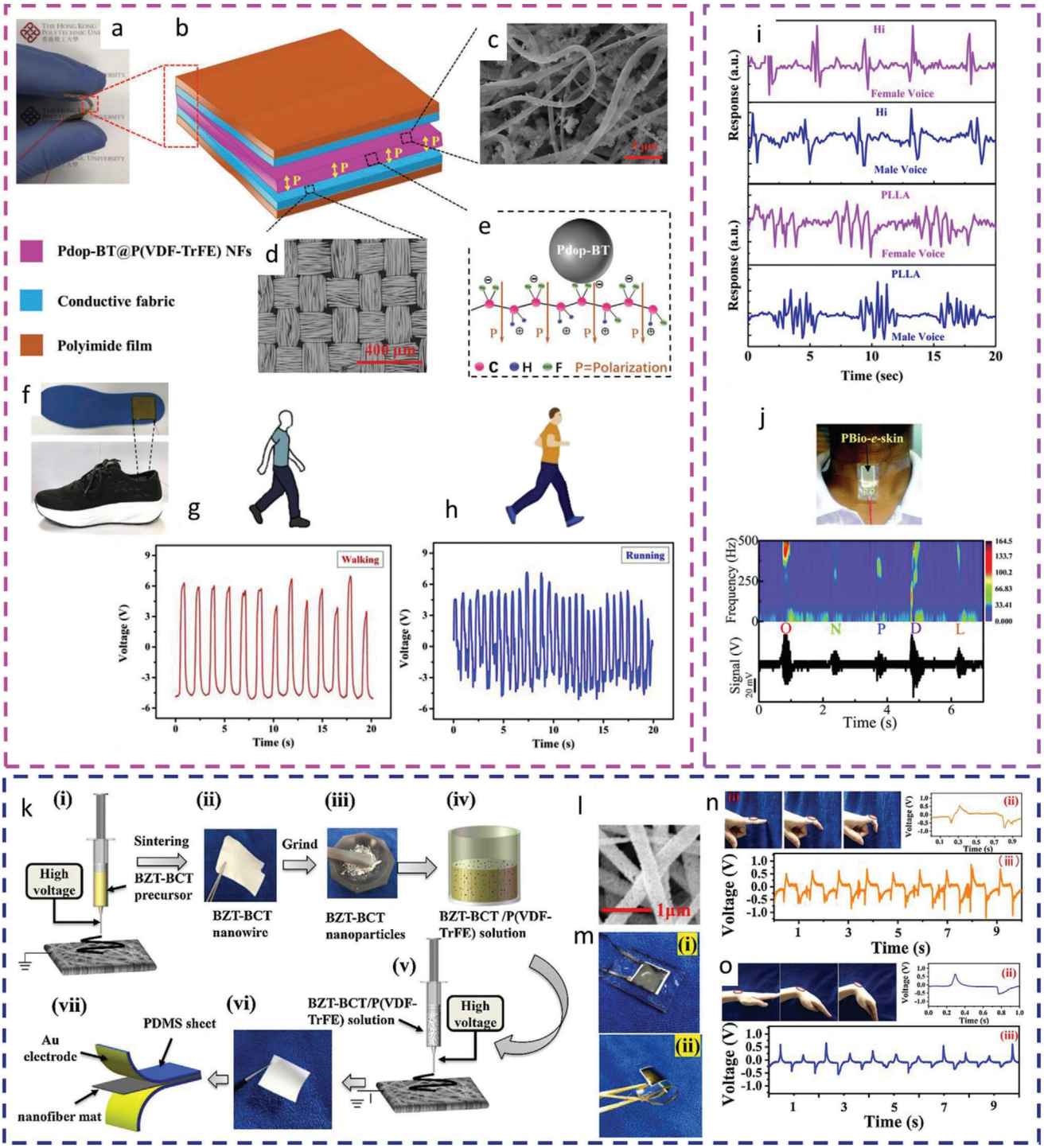

Figure 6. Flexible nanocomposite PENG. a) A photograph of Pdop-BT@P(VDF-TrFE) PENG. b) Schematic illustration of the PENG structure. c,d) SEM image of the surface morphology of Pdop-BT@P(VDF-TrFE) nanocomposite membrane and conducting fabric. e) Schematic illustration of the polarization direction. f) Photographs of PENG integrated into the insole of a shoe. g,h) The output voltages generated by walking and running, respectively. Reproduced with permission.[132] Copyright 2020, Elsevier Ltd.; i) Wavefront spectrum of female and male voices. j) Output wavefront spectrum observed from PBio-e-skin as different letters are pronounced with FFT signal in the upper part. Reproduced with permission.[139] Copyright 2017, The Royal Society of Chemistry.; k) Schematic diagram of the fabrication process of BZT-BCT/P(VDF-TrFE) PENG. l) SEM image of BZT-BCT nanowires. m) A photograph of BZT-BCT/P(VDF-TrFE) PENG. n,o) The output voltages generated from finger and wrist joint, respectively. Reproduced with permission.[130] Copyright 2020, Elsevier Ltd.

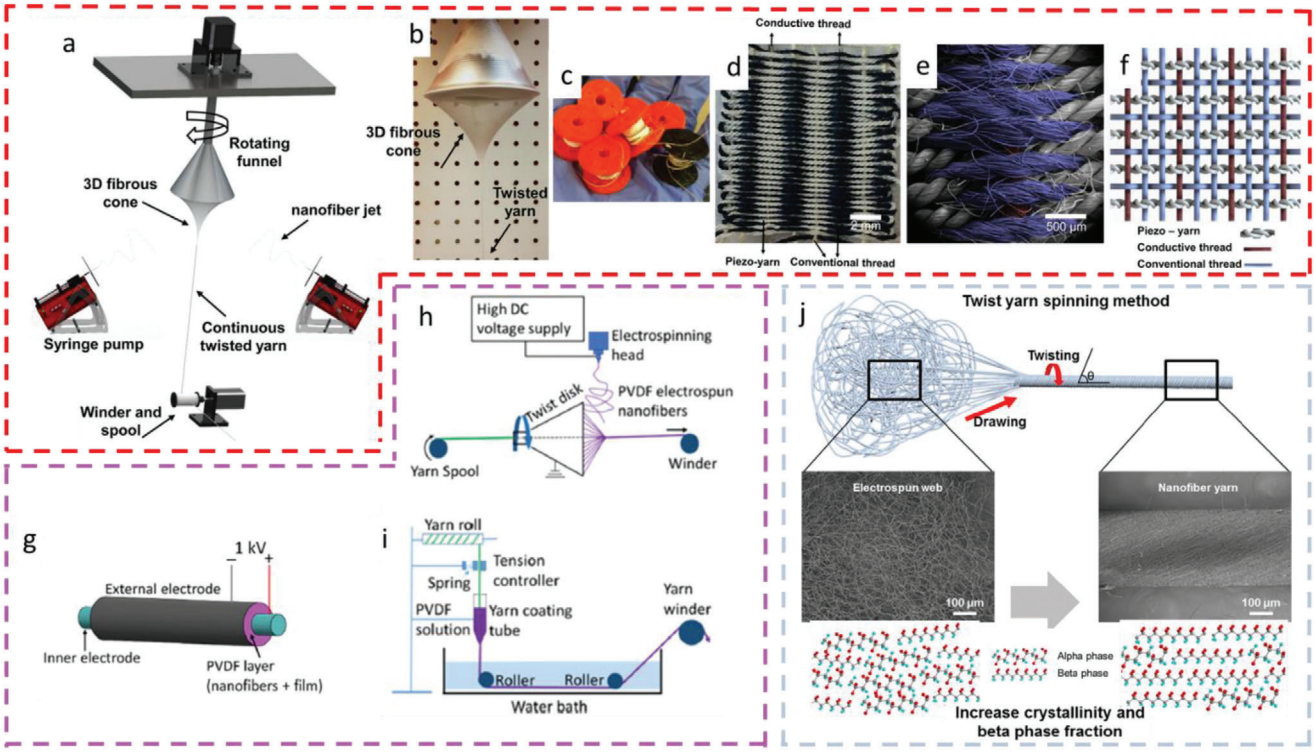

Figure 7. Electrospun piezoelectric fibers for functional smart textile yarns. a) Schematic of the apparatus for manufacturing of continuous twisted yarns. b) 3D fibrous cone and twisted yarn from this cone. c) Twisted yarns collected on spools. d) Photograph of a weaved piezoelectric fabric made of P(VDF-TrFE) yarns, conductive threads, and conventional threads. e) False-colored SEM image shows the fabric. f) Schematic shows the weave pattern of the piezoelectric fabric. Reproduced with permission.[144] Copyright 2017, American Chemical Society. g) Schematic of electrical poling for yarn. h,i) Schematics for deposition of PVDF nanofibers around conductive core yarn by electrospinning and coating of PVDF film, respectively. Reproduced with permission.[145] Copyright 2018, IOP Publishing Ltd. j) Schematic diagram of the twist-spinning technique and the resulting nanostructures of P(VDF-TrFE) nanofiber yarns. Reproduced with permission.[147] Copyright 2019, Elsevier Ltd.

movements. In addition, sound pressure below 120 dB could be harvested and as a result, 0.25 V output voltage was obtained.[150] Fuh et al. prepared piezoelectric PVDF NG by NFES and in situ poling on a flexible substrate. The integration of the three-layers of NG has achieved the maximum output voltage and current of 20 V and 0.390 μA, respectively.[151]

4.2. Triboelectric NGs

Triboelectrification term describes the tribology and electrostatic charge transfer process between the interfaces. The triboelectric NGs (TENGs) that convert mechanical energy into electricity using the combined effect of contact electrification and electrostatic induction were invented in 2012.[156] Contact electrification is the scientific term for triboelectrification meaning that mechanical friction is not required, the two different material surfaces are electrically charged as a result of physical contact.[157] The contact electrification allows the formation of opposite charges on the surface of two dissimilar materials. The relative positions of the charged surfaces change due to mechanical action, causing the induced potential difference between the electrodes to change. This change triggers the movement of free electrons at the electrodes, enabling the conversion of mechanical energy into electrical energy at high efficiency.

4.2.1. Triboelectric Materials Used in NGs

TENGs stand out with their ability to collect irregular and low-frequency mechanical energies, a wide range of materials used in their fabrication, easy fabrication at low cost, and lightweight. The capability of TENGs to sense and harvest mechanical energies such as human movements, vibration, and walking makes them suitable for wearable electronics applications. Four fundamental working modes of TENGs have been developed, which are vertical contact separation, lateral shear, single electrode, and independent triboelectric layer modes. The output performance of TENG is governed by the material and structural figure of merits. The material figure of merit is related to the surface charge density and the performance of TENG is proportional to its square.[158] It is known that the modifications of material surface through morphology and functionalization, choice of the triboelectric pairs, and thickness of the material influence the surface charge density.[108,159–163] Creating micro/nanostructures on the material surface contributes to the increase of surface charge density by extending the triboelectric contact area on the surface. Polymeric triboelectric material has an internal porous structure, charges are not only generated on the surface but also induced in the interior of the pores.[164–166] For the preparation of the triboelectric materials with micro/nanostructures, electrospinning is a timesaving, cost-effective, simple, and scalable technique

compared to lithography techniques such as photo-, nanoimprinting, and laser interference.[167–169] Electrospun fibers have an inherently rough and high specific surface area, as well as the surface and inner morphology of the fibers can be tailored in situ at the nanoscale.[79,170] The triboelectric series is a list used for the selection of triboelectric pairs in which materials are ordered according to their tendency to gain or lose electrons.[160,171,172] The further apart the two materials in the series are, the greater the charge transferred, resulting in higher TENG output performance. For instance, PVDF and its copolymers are among the most negative triboelectric materials due to their fluorine side chains and are extensively used in this field.[173–175]

4.2.2. Electrospun Fiber-Based TENGs

Electrospinning leads to the formation of the β-phase of PVDF by aligning polymers at the molecular level. Among the phases of the PVDF, the β-phase shows the greatest dipole moment due to the opposite direction arrangement of fluorine and hydrogen atoms. Hence, the polarity of the polymer increases and becomes much more negative.[176] Kong et al. prepared PVDF nanofibers with various surface morphology and β-phase ratio by regulating the kinetics of solvent evaporation at various relative humidity.[176] The increase in relative humidity from 10 to 70% caused the specific surface area to increase from 1.991 to 2.780 $m^2\ g^{-1}$ and the β-phase ratio to increase from about 70 to 95%. As a result of the increment in surface area and the β-phase, the output voltage, current, and output power increased from 14 to 234 V, 0.5 to 11 μA, and 5 to 1738 $\mu W\ cm^{-2}$, respectively. Zhang et al. fabricated TENG using nanoporous PVDF fibers as a negative polarity layer and elastic natural rubber as a positive polarity layer. The inner porous structure of PVDF fibers is controlled by varying the polymer concentration from 10 to 18 wt/v% in a mixture of dimethyl sulfoxide and acetone.[164] The specific surface area of the PVDF electrospun membrane increases from 6.9 to 11.0 $m^2\ g^{-1}$, resulting in an approximately 2.3-fold increase in output voltage. As aforementioned in the previous section, the β-phase ratio of the PVDF fiber can be enhanced by doping the inorganic nanoparticles to the polymer. Multi-walled carbon nanotube (MWCNT), Ag nanowire (AgNW), graphene quantum dot, iron (II, III) oxide (Fe_3O_4), ZnO, and TiO_2 nanoparticles are reported as doping materials.[7,177–183] Shaikh et al. used MWCNT to increase the β-phase content of PVDF fiber and triboelectric charge generation.[177] Incorporation of MWCNT at 1 wt% enhanced the peak-to-peak current output approximately from 0.004 to 0.016 μA. The PVDF fibers are woven with commercial nylon cloth and its application is demonstrated for body movements. Kim et al. fabricated a composite using P(VDF-TrFE) electrospun fiber and AgNWs for a self-powered wearable touch panel.[178] The output performance of TENG was improved by optimizing the concentration of AgNWs. The P(VDF-TrFE) fibers are inserted in the PDMS matrix to ensure mechanical stability and transparency. The device produced a power density of up to 21 700 $\mu W\ cm^{-2}$ outputs, with repeated contact and separation from the surface of a latex glove (**Figure 8**a–e).

The membranes fabricated by electrospinning have high air permeability, which is necessary for skin health due to its intrinsically porous structure that occurred by the pile-up of fibers.[162,184] Cao et al. fabricated a gas permeable self-powered triboelectric sensor for respiratory monitoring based on a PVDF nanofiber membrane and Ag nanoparticles electrode.[162] The permeability of the material is 6.16 $mm\ s^{-1}$, 4.5 times higher than paper and the output performance is reported to be stable for 30 min. Li et al. developed an all-fiber structured electronic skin with gas permeability and high flexibility.[184] The electronic skin is composed of three layers of electrospun nanofibers, namely, PVDF, carbon, and polyurethane (PU) nanofibers. This triple combination of the layers is designed as waterproof electrification, flexible electrode, and elastic substrate, respectively. Electrical output increased from 21.2 to 100.5 V when the area of electronic skin was increased from 1.0 to 9.0 cm^2 under a fixed 100 kPa external force. The skin was tested between 0 and 350 kPa and its sensitivity was designated as 0.18 $V\ kPa^{-1}$ in the sensing range of 0–175 kPa at a 1.0 cm^2.

In addition to PVDF and its copolymers, PAN (polyacrylonitrile), PVA (poly(vinyl alcohol), PDMS, PU, PLLA, PTFE (polytetrafluoroethylene), PMMA (poly(methyl methacrylate)), polyimide (PI), PA6, silk fibroin, and ethyl cellulose have also been reported for the fabrication of nanofiber-based wearable TENGs.[163,185–191] Jiang et al. have prepared an all-electrospun flexible TENG using PVA fiber doped with electronegative MXene nanosheets as a negative friction layer and silk nanofibers as a positive friction layer.[187] Proposed TENG can be used for both energy harvesting and real-time monitoring of body movement. It can support a high-power density of 108.76 $\mu W\ cm^{-2}$ with a 5.0 MΩ load resistance. Qui et al. designed a self-powered respiratory monitoring and finger-touch sensing sensor using polyaniline (PANI) fiber as an electrode layer, PVDF fiber as a negative layer, and PA6 as a positive layer (Figure 8f–h).[185] The output of TENG current and voltage can reach up to 200 μA and 1000 V, respectively. The application of the respiratory sensor has shown that voltage outputs that differ depending on the form of respiration such as normal, deep, rapid respiration, can be detected (Figure 8i–k).

4.3. Hybrid Piezoelectric-Triboelectric NGs

In most of the reported NG, mechanical energy was converted into electricity by a single conversion mechanism. However, using only one conversion mechanism causes large energy losses during the generation of electricity. Additionally, the detection of multiple stimulus types (stretching, bending, pressure, twisting, etc.) by self-powered sensors will lead to the widening of their applications. Using hybrid conversion mechanisms is one of the most efficient ways to achieve high energy conversion efficiency and high electrical performance from miniature devices.[192–195] Studies on the combination of triboelectric and piezoelectric effects have recently been reported for hybrid nanogenerators with high electrical efficiency and a wide range of measurements.

4.3.1. Materials Used in Hybrid NGs

As stated in the previous section, PVDF and its polymers of various comonomers have been preferred in both piezoelectric and triboelectric nanogenerators due to their high piezoelectric coefficient and negative surface polarity. Hence, they have been

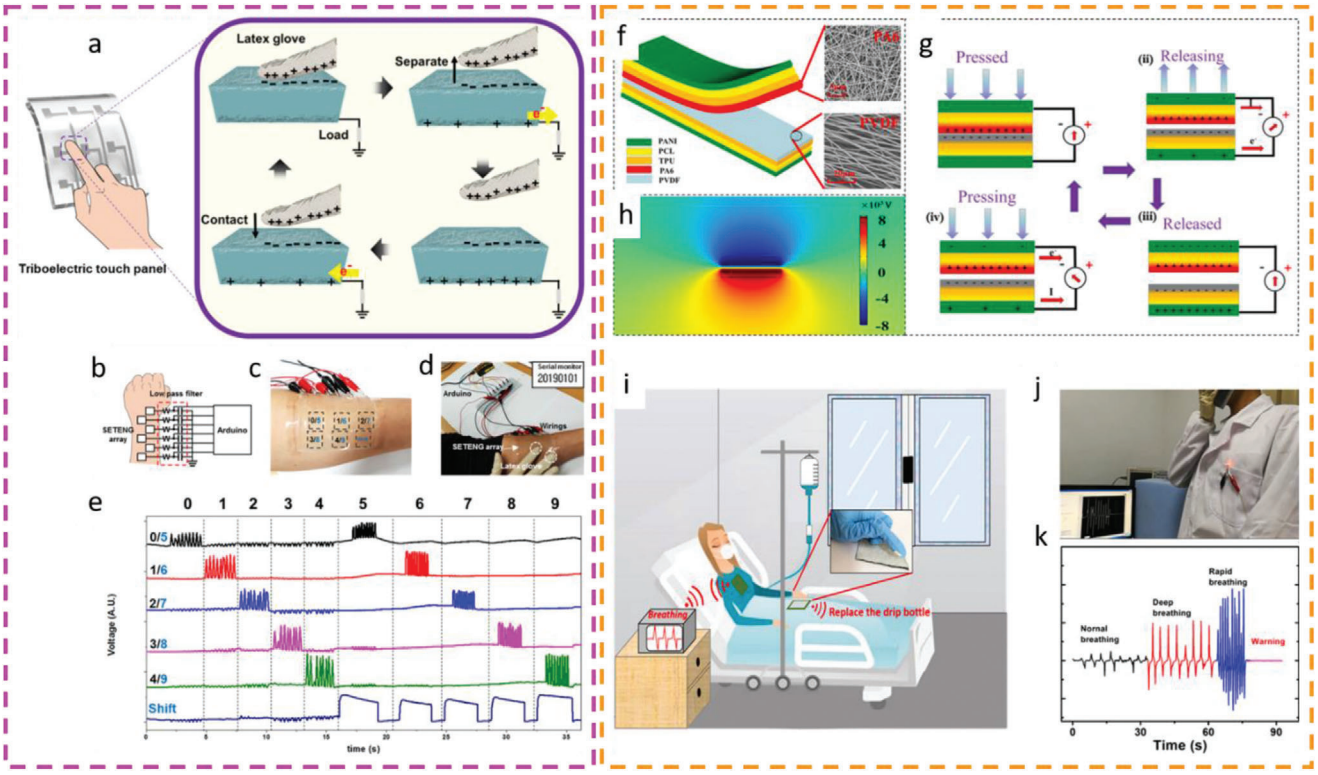

Figure 8. Flexible nanocomposite TENG. a) Schematic diagram of the TENG touch panel. b–d) Schematic of the touch panel circuit, key composition, and the photograph of the touch panel operation with PC and Arduino, respectively. e) Typed numbers from 0 to 9. Reproduced with permission.[178] Copyright 2019, American Chemical Society. f) Structure of the wearable designed TENG, and SEM image of nylon 6 (PA6) and PVDF nanofibers membrane. g) The working mechanism of the TENG. h) Simulation of the potential distribution between two triboelectric materials. i) Application of TENG for intensive care. j,k) Photograph of respiratory monitoring and the corresponding output current, respectively. Reproduced with permission.[185] Copyright 2019, Elsevier Ltd.

frequently used alone or in combination with inorganic materials such as carbon nanotube, $BaTiO_3$, $(BaCa)(ZrTi)O_3$ (BCZT), molybdenum disulfide (MoS_2), graphene in the fabrication of electrospinning based piezoelectric- triboelectric hybrid NGs (PTNGs).[197–201]

4.3.2. Electrospun Fiber-Based PTNGs

PTNGs can be designed as multilayer structures in which piezoelectric and triboelectric materials are individually synthesized or structures in which piezoelectric and triboelectric properties are combined in a single layer.[196–198] Guo et al. presented an all fiber-based hybrid NG composed of electrospun PVDF and silk fibroin onto conductive fabric.[202] The working principle of the piezoelectric enhanced triboelectric hybrid effect was investigated, and output performances were obtained with 500 V output voltage, 12 μA short circuit current, and 310 μW cm^{-2} power, respectively. Additionally, the real-time monitoring application of hybrid NG is shown. This microsystem detects body movements and sends an SOS message to the mobile phone when the user falls to the ground. Song et al. designed a highly flexible textile-based PTNG with separate piezoelectric and triboelectric layers.[199] The piezoelectric layer was fabricated by electrospinning of PVDF solution doped with $BaTiO_3$ powder and MWCNT, and the resulting non-woven membrane was used without the need for further polarization. For the triboelectric unit, the PDMS solution was doped with MWCNT and processed along with a sandpaper and a doctor blade to provide a microstructured surface. The conductive fabric was used as an electrode. Energy harvesting applications from human movements of PTNG placed on clothing were demonstrated and promising results were obtained. To demonstrate the application of energy harvesting from human movements, PTNG was placed in various areas of the garment and promising results were obtained. Approximately 162 V output voltage and 2.22 W electrical power density were produced from the 4.5×5 cm^2 area of the device. Furthermore, the experimental research was supported by finite element simulation and theoretical analysis.

PDMS is compatible with the skin surface due to its high deformity, gas permeability, inert, and nontoxic properties. Therefore, they are often preferred for nanogenerators encapsulation.[196,200,203] Yu et al. prepared piezoelectric-enhanced triboelectric nanogenerator from microfrustum arrays (m) polarized PZT-PDMS film, P(VDF-TrFE) nanofibers, and m-Cu film.[203] The triboelectric signal is generated as a result of contact–separation interaction between P(VDF-TrFE) nanofibers and m-Cu film, whereas piezoelectric signals are associated with the deformation of the polarized m-PZT-PDMS film. The proposed PTNG could sense weak and strong forces simultaneously and in real time. The triboelectric effect is pioneering in the range

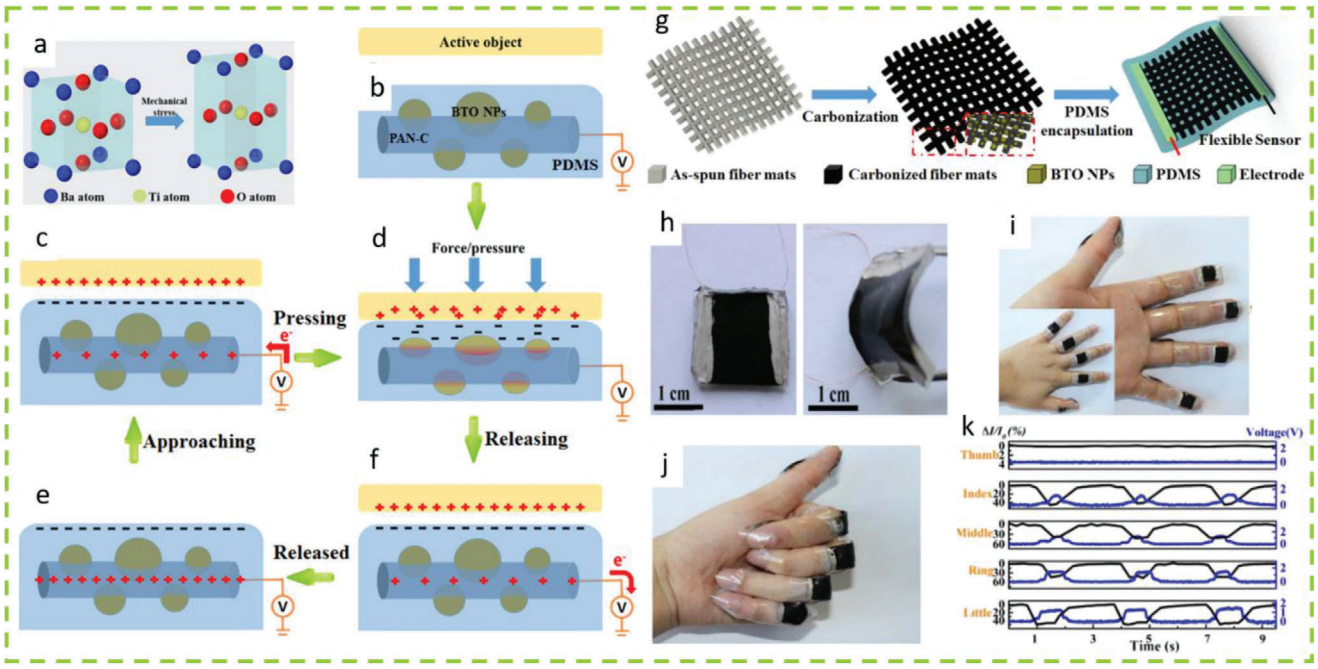

Figure 9. Piezoelectric-triboelectric hybrid NG. a–f) The working mechanism of the self-powered PAN-C/BTO-based sensor. g) Schematic representation of the fabrication process. h) Photograph of the self-powered sensor. i–k) The sensors on each finger show various hand gestures. Reproduced with permission.[196] Copyright 2018, American Chemical Society.

of 0–100 kPa and the sensitivity is up to 15.43 V kPa^{-1}. Both piezoelectric and triboelectric effects are active when the external force is in the range of 100–800 kPa, and sensitivity reaches up to 18.96 V kPa^{-1}. Zhao et al. fabricated a flexible self-powered sensor by combining piezoresistive, triboelectric, and piezoelectric effects in a single nanofiber film layer.[196] The sensor could independently and concurrently sense pressure and curvature. The film layer was formed by carbonization of $BaTiO_3$ doped as-spun PAN fiber and then encapsulated with PDMS. The incorporation of $BaTiO_3$ nanoparticles into the PAN nanofiber produces a synergistic effect of piezoelectric and triboelectric, which leads to an improvement in sensitivity over 2.4-fold (**Figure 9**). This result was also confirmed by a finite-element model. The curvature sensor can detect from 58.9 to 120.2° with an accuracy of 1.12 deg^{-1}. The gauge factor for the force sensor was 1.44 in the working range of 0.15–25 N. In addition, the sensor is extremely stable with over 60000 cycles when functioning in both modes.

5. Summary and Perspective

This study reviews the potential of wearable electronics in both industry and academia, the working principle of electrospinning, and the applications of electrospun materials in piezoelectric, triboelectric, and hybrid nanogenerators, focusing on the selected functional material. The place of wearable electronics in our daily life is increasing remarkably. This progress enables us to look out for basic issues such as health and safety while keeping up with the rapidly changing and developing digital world. Wearable electronics are expected to be flexible, stretchable, and miniature to allow users to perform their daily movements comfortably, otherwise will be resulted in ineffective use.

The lack of flexibility and continuous need of charging for three existing batteries make them inadequate for wearable electronic applications. Therefore, being supported by a flexible, uninterrupted, and sustainable power supply is an important step that will increase their rapid spread. Harvesting mechanical energy arising from human movements and converting it into electricity with nanogenerators is a powerful alternative for providing of uninterrupted energy supply for wearable electronic devices. In the last decay, the wearable electronic applications of nanogenerators have attracted the attention of many researchers and the studies on this subject have increased significantly.

Fiber-based nanogenerators have been standing out for their flexibility and large surface area advantages. Electrospinning is one of the most preferred simple fiber production techniques that come forward for its adaptability, cost-effectiveness, and efficiency. 2D nanofibers and 3D macrostructures of exceptional length with a uniform diameter can be produced by electrospinning. The surface and internal structure morphology of the fibers can also be controlled with this technique and the material can be aligned at the molecular level. Many fiber fabrication technologies such as NFES, hydrodynamic writing, multineedle or needle-free electrospinning, coaxial electrospinning, electroblowing, melt spinning, bubble electrospinning, conjugate electrospinning, emulsion electrospinning, wet spinning have been developed by changing the injection and collection systems of electrospinning in different ways. All of these features have shown that electrospun fibers are suitable materials for energy harvesting applications in wearable electronics.

The processing method, selected functional materials, output performance, and detection/application type of electrospun fiber-based NGs, are presented in **Table 1**. Also, the electrospun

Table 1. Shortlist of electrospun fiber-based NGs reported in the literature.

Processing method	Functional material	Area, applied force and type, frequency	Voltage, current, power output	Types of sensing/application	Stability	Refs.
Piezoelectric nanogenerators						
Solution electrospinning	PVDF fiber	15 mm × 10 mm, 20 N and tapping, 1 Hz	0.91 μW	–		[114]
Solution electrospinning	PVDF fiber	42 mm × 20 mm × 0.6 mm, 37 N and bending, 1.4 Hz	1.5 V, 0.4 μA	Vocal cord vibrations, respiration monitoring, subtle muscle movement		[117]
Solution electrospinning	PVDF fiber	40 mm × 50 mm × 2 mm, 12 N, 0.07 Hz	≈0.0045 V	Bending, walking, running		[118]
Solution electrospinning	PVDF/TiO_2 fiber	9.0 cm × 7.5 cm with 250 μm thickness, ≈5 N and tapping	11.5 V, 0.176 μA	Walking, running, jumping, acoustic vibration	2000 s	[9]
Solution electrospinning/ Hydrothermal method	PVDF-HFP/Co-ZnO	2.5 N and tapping, 50 Hz	2.8 V	Stretching, bending, twisting		[122]
Solution electrospinning/ Solvothermal method	PVDF/ ZnO nanorods	Bending, ≈4 Hz	85 V, 2.2 μA	Finger bending		[123]
Solution electrospinning	PVDF/ PANI/ g-C_3N_4	5.5 cm^2, punching	≈30 V, 3.7 μA, 14.7 μW cm^{-2}	Pressing, bending	>50000 cycle	[124]
Solution electrospinning	PVDF/Ag	20 mm × 40 mm with 100 μm thickness, air flow, and bending, 0.5 Hz	≈4.6 V	Respiratory monitoring	6000 s	[125]
Solution electrospinning	BZT-BCT/P(VDF-TrFE)	1 × 1 cm^2, 6 N and tapping, 10 Hz	13.01 V, 1.44 μW	Tapping, bending	5000 cycle	[130]
Solution electrospinning/surface adsorption	Pdop-$BaTiO_3$ @ P(VDF-TrFE)	2.5 cm × 2.5 cm, 700 N and pressing, 2 Hz	6 V, 1.5 μA, ≈0.878 μW cm^{-2}	Squatting walking running	10 000 cycle	[132]
Solution electrospinning	BNT-ST/ P(VDF-TrFE)	47.77 kPa and pressing	0.181 V	Bending running walking		[146]
Near-field electrospinning	PVDF	1 × 1 cm^2, finger pressing	4 V, 0.1 μA	Bending striking motions	≈3000 cycles	[151]

(*Continued*)

Table 1. Continued.

Processing method	Functional material	Area, applied force and type, frequency	Voltage, current, power output	Types of sensing/application	Stability	Refs.
Triboelectric nanogenerators						
Solution electrospinning, cold pressing	PLLA (−) Ethyl cellulose (+)	2 cm × 2 cm, 3.5 Hz	19 V, 0.630 μA	Human walking, limbs motion	6000 cycles	[163]
Solution electrospinning	PVDF (−) Nature rubber (+)	45 mm ×45 mm, 5.6 N, 5 Hz	1222 V, 132 μA	Running, Walking, Squatting		[164]
Coaxial electrospinning	PVDF (−) PHBV (+)	45 mm × 55 mm, 2 Hz	1000 V, 90 μA, 600 μW cm^{-2}	–		[166]
Solution electrospinning	P(VDF-HFP) (−) Nylon 6 (+)	4 cm × 4 cm	≈300 V, ≈14 μA	Bending, pressing, touching	1600 cycles	[174]
Solution electrospinning	PVDF (−) Al foil (+)	1 cm × 1 cm	234 V, 11 μA, 1738 μW cm^{-2}	–	5000 cycles	[176]
Solution electrospinning	P(VDF-TrFE)/AgNW (−) Latex glove (+)	1 cm^2, 3 Hz	150 V, 90 μA	Touch panel	10000 cycles	[178]
Solution electrospinning	PVDF/GQD (−) Al foil (+)	6 cm × 6 cm	≈110 V, ≈3.5 μA, 97 μW	–		[180]
Solution electrospinning	PVA/MXene (−) silk (+)	28 cm^2, 10 N and pressing, 10 Hz	≈53 V, ≈15 μA, 108.76 μW cm^{-2}	Real-time human activity monitoring	12 4000 cycles	[187]
Coaxial electrospinning	PDMS ion gel/ P(VDF-HFP) (+) Kapton (−)	700 kPa and pressing, 5 Hz	≈70 V, 9 μA cm^{-2}	Heart rate monitoring		[188]
Emulsion electrospinning	PTFE (−) PA6 (+)	2 cm × 2 cm, 50 N and squeezing, 5 Hz	≈900 V, ≈20000 μA m^{-2}, ≈900 μW cm^{-2}	–	30 000 cycles	[190]
Solution electrospinning	PVDF (−) PA6 (+)	80 mm × 40 mm, 2.5 Hz	1000 V, 200 μA, 1717 μW cm^{-2}	Health monitoring	5500 cycles	[185]
Hybrid nanogenerators						
Solution electrospinning	Carbonized PAN/$BaTiO_3$	1.5 cm × 1.5 cm, 25 N and pressing	49 V, 0.48 μA	Swallowing, walking, finger flexure, and finger-tapping	60000 cycles	[196]
Solution electrospinning	BCZT/P(VDF-HFP) (+) Silicon rubber (-)	2 cm × 2 cm, ≈8 N and pressing	16.17 μW cm^{-2}	Finger tapping and bending, hand touching	1200 cycles	[197]
Solution electrospinning	PVDF-CNT-$BaTiO_3$ PDMS-MCNT-graphite (−) Conductive fabric (+)	4.5 cm × 5 cm, 580 N and pressing, 3.3 Hz	161.66 V, 222 μW cm^{-2}	Footstep, clapping, body movement	5000 cycles	[199]
Solution electrospinning	PVDF (−) silk fibroin/PEO (+)	2 cm × 4 cm, ≈25.7 N and pressing, 2 Hz	500 V, 12 μA, 310 μW cm^{-2}	Body motion	10000 cycles	[202]
Solution electrospinning, grinding	P(VDF-TrFE) (−) m-Cu (+) m-PZT-PDMS	18 mm × 20 mm, 1300 kPa and pressing	≈180 V, 2.250 μA	Pulse wave, body movement	100000 cycles	[203]

Macromolecular Materials and Engineering
www.mame-journal.de

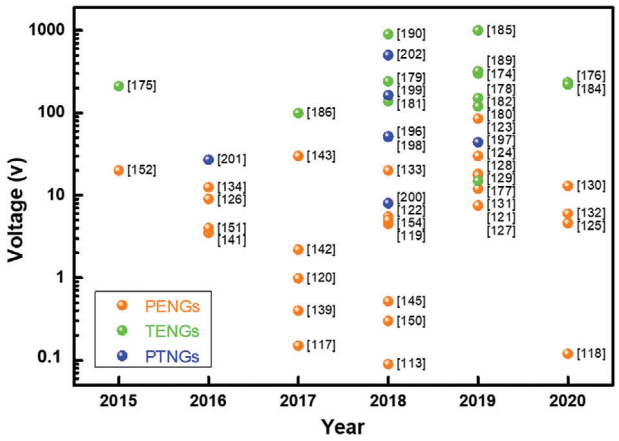

Figure 10. Summary of electrospun fiber-based NGs reported in last five years. TENGs and PTNGs data are given as y offsets +1 and +2, respectively.

fiber-based NGs reported in the last five years are summarized in **Figure 10**. Energy generation and conversion efficiency in PENGs, TENGs, and PTNGs largely depend on material design and structure. Micro and nano-structured materials with high specific surface area contribute greatly to this purpose. Electrospun PVDF and its copolymers are the most preferred polymers in both piezoelectric and triboelectric nanogenerator studies. The polar β-phase crystal structure of PVDF can be enhanced by methods that can be easily achieved by electrospinning such as mechanical stretching, exposure to a strong electrical field, and doping with inorganic nanofillers. In piezoelectric nanogenerator studies, PVDF polymers are often doped with inorganic nanoparticles with high piezoelectric coefficients to obtain more functional and efficient materials. Studies have shown that the amounts of the additive have been affected the morphology of the β-phase of the material. There is a percolation threshold for the amount of doping required to obtain maximum β-phase content. Compared to other nanogenerators, TENGs stand out with their ability to collect irregular and low-frequency mechanical energies. It is possible to increase the charge density on the surface of the material by using electrospun fibers with a porous surface and internal structure and applying surface modification. It also contributes positively to the triboelectric effect, the polarity of PVDF polymers increases with the increase of beta phase. The application areas of PTNGs are expanding due to the widening of the force range perceived by the device and their ability to detect various types of excitation forces.

Even though electrospun-based nanogenerators have the potential to be a suitable power source for wearable electronic devices, they will still need further study for practical implementation. In the near future, the way to develop more functional and innovative materials will be clarified using the adaptability and morphology control feature of the electrospinning technique. The innovative fiber-based materials enable to obtain higher output performance nanogenerators. However, in long-term use, electrospun fibers may deform and disrupt the stability of the device. For this reason, the material design should be considered as an important parameter for high stability devices. In addition, a systematic study is needed on the use of nanogenerators in wearable electronics in practice and on the determination of operating conditions. Taking these challenges into account will open new doors and contribute to the acceleration of developments in this highly demanded subject.

The rapid growth of the market in wearable electronics, as demonstrated by the analysis, has revealed potential in this area. These developments in wearable electronics are expected to be accelerated by the successful integration of electrospun material-based self-power sensors/nanogenerators. It is inevitable that these revolutionary technologies, which will make our life easier in many ways and improve our quality of life, are indispensable parts of our daily life.

Conflict of Interest

The authors declare no conflict of interest.

Keywords

energy harvesting, piezoelectric nanogenerators, self-powered sensors, smart textiles, triboelectric nanogenerators

Received: March 2, 2021
Revised: April 13, 2021
Published online:

[1] X. Pu, Z. L. Wang, *Chem. Sci.* **2021**, *12*, 34.
[2] Z. L. Wang, J. Song, *Science* **2006**, *312*, 242.
[3] Y. Zi, Z. L. Wang, *APL Mater.* **2017**, *5*, 074103.
[4] G. Kalimuldina, N. Turdakyn, I. Abay, A. Medeubayev, A. Nurpeissova, D. Adair, Z. Bakenov, *Sensors* **2020**, *20*, 5214.
[5] L. Persano, A. Camposeo, C. Tekmen, D. Pisignano, *Macromol. Mater. Eng.* **2013**, *298*, 504.
[6] L. Yu, P. Zhou, D. Wu, L. Wang, L. Lin, D. Sun, *Microsyst. Technol.* **2018**, *25*, 3151.
[7] X. Pu, J.-W. Zha, C.-L. Zhao, S.-B.o Gong, J.-F. Gao, R. K. Y. Li, R. K. Y. Li, *Chem. Eng. J.* **2020**, *398*, 125526.
[8] M. S. Sorayani Bafqi, R. Bagherzadeh, M. Latifi, *J. Polym. Res.* **2015**, *22*, 130.
[9] M.d. M. Alam, A. Sultana, D. Mandal, D. Mandal, *ACS Appl. Energy Mater.* **2018**, *1*, 3103.
[10] Wearable Electronics Market by Product and Geography – Forecast and Analysis 2020–2024. **2020**. https://www.technavio.com/report/wearable-electronics-market-industry-analysis (accessed: April 2021).
[11] R. Singh, Wearable Electronics Market Overview. **2014**. https://www.alliedmarketresearch.com/body-adapted-wearable-electronics-market (accessed: April 2021).
[12] A. Nozariasbmarz, H. Collins, K. Dsouza, M. H. Polash, M. Hosseini, M. Hyland, J. Liu, A. Malhotra, F. M. Ortiz, F. Mohaddes, V. P. Ramesh, Y. Sargolzaeiaval, N. Snouwaert, M. C. Özturk, D. Vashaee, *Appl. Energy* **2020**, *258*, 114069.
[13] W. Zeng, L. Shu, Q. Li, S. Chen, F. Wang, X.-M. Tao, *Adv. Mater.* **2014**, *26*, 5310.
[14] J. H. Koo, D. C. Kim, H. J. Shim, T.-H. Kim, D.-H. Kim, *Adv. Funct. Mater.* **2018**, *28*, 1801834.
[15] Z. Lou, L. Wang, K. Jiang, Z. Wei, G. Shen, *Mater. Sci. Eng., R* **2020**, *140*, 100523.
[16] H.-R. Lim, H. S. Kim, R. Qazi, Y.-T. Kwon, J.-W. Jeong, W.-H. Yeo, *Adv. Mater.* **2020**, *32*, 1901924.

[17] A. Chinnappan, C. Baskar, S. Baskar, G. Ratheesh, S. Ramakrishna, *J. Mater. Chem. C* **2017**, *5*, 12657.
[18] C. Wang, K. Xia, H. Wang, X. Liang, Z. Yin, Y. Zhang, *Adv. Mater.* **2019**, *31*, 1801072.
[19] L. Wang, M. Zhang, B. Yang, X. Ding, J. Tan, S. Song, J. Nie, *ACS Appl. Mater. Interfaces* **2021**, 13, 5486.
[20] X. Chen, *Small Methods* **2017**, *1*, 1600029.
[21] B. Wang, A. Facchetti, *Adv. Mater.* **2019**, *31*, 1901408.
[22] J. A. Rogers, T. Someya, Y. Huang, *Science* **2010**, *327*, 1603.
[23] H. Jang, Y. J. Park, X. Chen, T. Das, M.-S. Kim, J.-H. Ahn, *Adv. Mater.* **2016**, *28*, 4184.
[24] Y. Liu, M. Pharr, G. A. Salvatore, *ACS Nano* **2017**, *11*, 9614.
[25] N. Matsuhisa, X. Chen, Z. Bao, T. Someya, *Chem. Soc. Rev.* **2019**, *48*, 2946.
[26] Y. Liu, K. He, G. Chen, W. R. Leow, X. Chen, *Chem. Rev.* **2017**, *117*, 12893.
[27] L. Huang, S. Lin, Z. Xu, H.e Zhou, J. Duan, B. Hu, J. Zhou, *Adv. Mater.* **2020**, *32*, 1902034.
[28] X. Guan, B. Xu, M. Wu, T. Jing, Y. Yang, Y. Gao, *Nano Energy* **2021**, *80*, 105549.
[29] K. Dong, X. Peng, Z. L. Wang, *Adv. Mater.* **2020**, *32*, 1902549.
[30] S. Günes, H. Neugebauer, N. S. Sariciftci, *Chem. Rev.* **2007**, *107*, 1324.
[31] S. B. Riffat, X. Ma, *Appl. Therm. Eng.* **2003**, *23*, 913.
[32] D. Champier, *Energy Convers. Manage.* **2017**, *140*, 167.
[33] R. A. Bullen, T. C. Arnot, J. B. Lakeman, F. C. Walsh, *Biosens. Bioelectron.* **2006**, *21*, 2015.
[34] G. Xue, Y. Xu, T. Ding, J. Li, J. Yin, W. Fei, Y. Cao, J. Yu, L. Yuan, L. Gong, J. Chen, S. Deng, J. Zhou, W. Guo, *Nat. Nanotechnol.* **2017**, *12*, 317.
[35] P. Tao, G. Ni, C. Song, W. Shang, J. Wu, J. Zhu, G. Chen, T. Deng, *Nat. Energy* **2018**, *3*, 1031.
[36] Z. L. Wang, W. Wu, *Angew. Chem., Int. Ed.* **2012**, *51*, 11700.
[37] G. Tan, L.i-D. Zhao, M. G. Kanatzidis, *Chem. Rev.* **2016**, *116*, 12123.
[38] C. Wu, A. C. Wang, W. Ding, H. Guo, Z. L. Wang, *Adv. Energy Mater.* **2019**, *9*, 1802906.
[39] M. Thielen, L. Sigrist, M. Magno, C. Hierold, L. Benini, *Energy Convers. Manage.* **2017**, *131*, 44.
[40] P. Yang, K. Liu, Q. Chen, X. Mo, Y. Zhou, S. Li, G. Feng, J. Zhou, *Angew. Chem., Int. Ed.* **2016**, *55*, 12050.
[41] G. Ward, *Filtr. Sep.* **2001**, *38*, 42.
[42] C. R. Martin, *Chem. Mater.* **1996**, *8*, 1739.
[43] J. D. Hartgerink, *Science* **2001**, *294*, 1684.
[44] G. Liu, L. Qiao, A. Guo, *Macromolecules* **1996**, *29*, 5508.
[45] P. X. Ma, R. Zhang, *J. Biomed. Mater. Res.* **1999**, *46*, 60.
[46] H. Niu, H. Zhou, H. Wang, in *Energy Harvesting Properties of Electrospun Nanofibers* (Eds: J. Fang, T. Lin), IOP Publishing, Bristol, UK **2019**, p. 20191. .
[47] Z.-M. Huang, Y. Z. Zhang, M. Kotaki, S. Ramakrishna, *Compos. Sci. Technol.* **2003**, *63*, 2223.
[48] A. Frenot, I. S. Chronakis, *Curr. Opin. Colloid Interface Sci.* **2003**, *8*, 64.
[49] D. H. Reneker, I. Chun, *Nanotechnology* **1996**, *7*, 216.
[50] D. Li, Y. Xia, *Adv. Mater.* **2004**, *16*, 1151.
[51] I. Han, K. J. Shim, J. Y. Kim, S. U. Im, Y. K. Sung, M. Kim, I.-K. Kang, J. C. Kim, *Artif. Organs* **2007**, *31*, 801.
[52] H. Powell, D. Supp, S. Boyce, *Biomaterials* **2008**, *29*, 834.
[53] R. Barhate, S. Ramakrishna, *J. Membr. Sci.* **2007**, *296*, 1.
[54] T. Isık, M. M. Demir, *Fibers Polym.* **2018**, *19*, 767.
[55] B. Satilmis, T. Isık, M. M. Demir, T. Uyar, *Appl. Surf. Sci.* **2019**, *467-468*, 648.
[56] Y. Liu, Y. Sun, H. Yan, X. Liu, W. Zhang, Z. Wang, X. Jiang, *Small* **2012**, *8*, 676.
[57] B. Sun, Y. Z. Long, H. D. Zhang, M. M. Li, J. L. Duvail, X. Y. Jiang, H. L. Yin, *Prog. Polym. Sci.* **2014**, *39*, 862.
[58] H. Yuce, T. Guner, S. Dartar, B. U. Kaya, M. Emrullahoglu, M. M. Demir, *Dyes Pigm.* **2020**, *173*, 107932.
[59] T. Guner, H. Yuce, D. Tascioglu, E. Simsek, U. Savaci, A. Genc, S. Turan, M. M. Demir, *Beilstein J. Nanotechnol.* **2019**, *10*, 2004.
[60] B. Ding, M. Wang, X. Wang, J. Yu, G. Sun, *Mater. Today* **2010**, *13*, 16.
[61] E. Inci, G. Topcu, T. Guner, M. Demirkurt, M. M. Demir, *J. Mater. Chem. C* **2020**, *8*, 12036.
[62] A. İncel, C. Varlikli, C. D. Mcmillen, M. M. Demir, *J. Phys. Chem. C* **2017**, *121*, 11709.
[63] P. S. Kumar, J. Sundaramurthy, S. Sundarrajan, V. J. Babu, G. Singh, S. I. Allakhverdiev, S. Ramakrishna, *Energy Environ. Sci.* **2014**, *7*, 3192.
[64] L. Dimesso, C. Spanheimer, W. Jaegermann, Y. Zhang, A. L. Yarin, *J. Appl. Phys.* **2012**, *111*, 064307.
[65] F. Anton, US1975504A, **1934**.
[66] W. Gilbert, *De Magnete*, Courier Corporation, Chelmsford, MA **1958**.
[67] G. I. Taylor, *Proc. R. Soc. London, Ser. A* **1964**, *280*, 383.
[68] D. H. Reneker, A. L. Yarin, H. Fong, S. Koombhongse, *J. Appl. Phys.* **2000**, *87*, 4531.
[69] M. M. Hohman, M. Shin, G. Rutledge, M. P. Brenner, *Phys. Fluids* **2001**, *13*, 2201.
[70] M. M. Demir, I. Yilgor, E. Yilgor, B. Erman, *Polymer* **2002**, *43*, 3303.
[71] Y. M. Shin, M. M. Hohman, M. P. Brenner, G. C. Rutledge, *Polymer* **2001**, *42*, 09955.
[72] E. Biber, G. Gündüz, B. Mavis, U. Colak, *Appl. Phys. A* **2010**, *99*, 477.
[73] H. Shao, J. Fang, H. Wang, C. Lang, T. Lin, *ACS Appl. Mater. Interfaces* **2015**, *7*, 22551.
[74] X. Wang, H. Niu, T. Lin, X. Wang, *Polym. Eng. Sci.* **2009**, *49*, 1582.
[75] H. Niu, T. Lin, X. Wang, *J. Appl. Polym. Sci.* **2009**, *114*, 3524.
[76] V. Beachley, X. Wen, *Mater. Sci. Eng., C* **2009**, *29*, 663.
[77] C. Ribeiro, V. Sencadas, J. L. G. Ribelles, S. Lanceros-Méndez, *Soft Mater.* **2010**, *8*, 274.
[78] X.-P. Tang, N. Si, L. Xu, H.-Y. Liu, *Therm. Sci.* **2014**, *18*, 1447.
[79] T. Isık, M. M. Demir, *Sustainable Mater. Technol.* **2018**, *18*, e00084.
[80] H. Begum, K. Khan, *Int. J. Text. Sci.* **2017**, *6*, 110.
[81] J. S. Kim, D. H. Reneker, *Polym. Eng. Sci.* **1999**, *39*, 849.
[82] P. Katta, M. Alessandro, R. D. Ramsier, G. G. Chase, *Nano Lett.* **2004**, *4*, 2215.
[83] D. Li, Y. Wang, Y. Xia, *Nano Lett.* **2003**, *3*, 1167.
[84] S. Nagam Hanumantharao, S. Rao, *Fibers* **2019**, *7*, 66.
[85] K. E. Gutowski, G. A. Broker, H. D. Willauer, J. G. Huddleston, R. P. Swatloski, J. D. Holbrey, R. D. Rogers, *J. Am. Chem. Soc.* **2003**, *125*, 6632.
[86] S.-L. Quan, S.-G. Kang, I.-J. Chin, *Cellulose* **2010**, *17*, 223.
[87] D. Yang, B. Lu, Y. Zhao, X. Jiang, *Adv. Mater.* **2007**, *19*, 3702.
[88] J. W. Lee, *J. Nanomater.* **2015**, *2015*, 213521.
[89] D. Sun, C. Chang, S. Li, L. Lin, *Nano Lett.* **2006**, *6*, 839.
[90] D. Di Camillo, V. Fasano, F. Ruggieri, S. Santucci, L. Lozzi, A. Camposeo, D. Pisignano, *Nanoscale* **2013**, *5*, 11637.
[91] X. Shi, W. Zhou, D. Ma, Q. Ma, D. Bridges, Y. Ma, A. Hu, *J. Nanomater.* **2015**, *2015*, 140716.
[92] D. Li, Y. Xia, *Nano Lett.* **2004**, *4*, 933.
[93] Z. Sun, E. Zussman, A. L. Yarin, J. H. Wendorff, A. Greiner, *Adv. Mater.* **2003**, *15*, 1929.
[94] F. Sun, S.-Y. Huang, H.-T. Ren, T.-T. Li, Y. Zhang, C.-W. Lou, J.-H. Lin, *Polym. Compos.* **2020**, *41*, 1013.
[95] A. L. Yarin, *Polym. Adv. Technol.* **2011**, *22*, 310.
[96] J. Yoon, H.-S. Yang, B.-S. Lee, W.-R. Yu, *Adv. Mater.* **2018**, *30*, 1704765.
[97] Y. Lin, Y.-Y. Yao, X.-Z. Yang, L.-M. Shen, R.-X. Li, D.-C. Wu, *Chin. J. Polym. Sci.* **2009**, *27*, 511.
[98] J. H. He, *Acta Phys. Pol., A* **2012**, *121*, 254.

[99] J. - H. He, Y. Liu, L. Xu, *Mater. Sci. Technol.* **2010**, *26*, 1275.
[100] X. Li, J. Qiang, Y. Wan, H. Wang, W. Gao, *J. Low Freq. Noise Vib. Act. Control* **2019**, *38*, 1246.
[101] Y. Wu, J.-Y. Yu, J.-H. He, Y.-Q. Wan, *Chaos, Solitons Fractals* **2007**, *32*, 5.
[102] S. Chandrasekaran, C. Bowen, J. Roscow, Y. Zhang, D. K. Dang, E. J. Kim, R. D. K. Misra, L. Deng, J. S. Chung, S. H. Hur, *Phys. Rep.* **2019**, *792*, 1.
[103] Z. L. Wang, J. Chen, L. Lin, *Energy Environ. Sci.* **2015**, *8*, 2250.
[104] G. Zhu, B. Peng, J. Chen, Q. Jing, Z. Lin Wang, *Nano Energy* **2015**, *14*, 126.
[105] S. Santangelo, *Appl. Sci.* **2019**, *9*, 1049.
[106] Z. Dong, S. J. Kennedy, Y. Wu, *J. Power Sources* **2011**, *196*, 4886.
[107] S. Tiwari, A. Gaur, C. Kumar, P. Maiti, *Energy* **2019**, *171*, 485.
[108] Z. Li, J. Shen, I. Abdalla, J. Yu, B. Ding, *Nano Energy* **2017**, *36*, 341.
[109] Z. L. Wang, *Nanogenerators for Self-Powered Devices and Systems*, Georgia Institute of Technology **2011**, http://hdl.handle.net/1853/39262 (accessed: April 2021).
[110] Z. L. Wang, *Nano Energy* **2020**, *68*, 104272.
[111] S. K. Ghosh, D. Mandal, D. Mandal, *Nano Energy* **2018**, *53*, 245.
[112] M. M. Alam, S. K. Ghosh, A. Sultana, D. Mandal, *ACS Sustainable Chem. Eng.* **2018**, *6*, 292.
[113] S. Ma, T. Ye, T. Zhang, Z. Wang, K. Li, M. Chen, J. Zhang, Z. Wang, S. Ramakrishna, L. Wei, *Adv. Mater. Technol.* **2018**, *3*, 1800033.
[114] P. K. Szewczyk, A. Gradys, S. Kim, L. Persano, M. M. Marzec, A. P. Kryshtal, T. Busolo, A. Toncelli, D. Pisignano, A. Bernasik, S. Kar-Narayan, P. Sajkiewicz, U. Stachewicz, *ACS Appl. Mater. Interfaces* **2020**, *12*, 13575.
[115] C. Chang, V. H. Tran, J. Wang, Y.-K. Fuh, L. Lin, *Nano Lett.* **2010**, *10*, 726.
[116] C. Wan, C. R. Bowen, *J. Mater. Chem. A* **2017**, *5*, 3091.
[117] Z. Liu, S. Zhang, Y. M. Jin, H. Ouyang, Y. Zou, X. X. Wang, L. X. Xie, Z. Li, *Semicond. Sci. Technol.* **2017**, *32*, 064004.
[118] Q. Liu, X.-X. Wang, W.-Z. Song, H.-J. Qiu, J. Zhang, Z. Fan, M. Yu, Y.-Z. Long, *ACS Appl. Mater. Interfaces* **2020**, *12*, 8288.
[119] Z. He, B. Gao, T. Li, J. Liao, B. Liu, X. Liu, C. Wang, Z. Feng, Z. Gu, *ACS Sustainable Chem. Eng.* **2018**, *7*, 1745.
[120] M. S. Sorayani Bafqi, R. Bagherzadeh, M. Latifi, *J. Ind. Text.* **2017**, *47*, 535.
[121] S. You, L. Zhang, J. Gui, H. Cui, S. Guo, *Micromachines* **2019**, *10*, 302.
[122] H. Parangusan, D. Ponnamma, M. A. Al-Maadeed, *Sci. Rep.* **2018**, *8*, 754.
[123] J. Li, S. Chen, W. Liu, R. Fu, S. Tu, Y. Zhao, L. Dong, B. Yan, Y. Gu, *J. Phys. Chem. C* **2019**, *123*, 11378.
[124] M. Khalifa, S. Anandhan, *ACS Appl. Nano Mater.* **2019**, *2*, 7328.
[125] L. Jin, Y. Zheng, Z. Liu, J. Li, H. Zhai, Z. Chen, Y. Li, *ACS Appl. Mater. Interfaces* **2020**, *12*, 1359.
[126] P. Adhikary, A. Biswas, D. Mandal, D. Mandal, *Nanotechnology* **2016**, *27*, 495501.
[127] M. Khalifa, A. Mahendran, S. Anandhan, *J. Polym. Res.* **2019**, *26*, 73.
[128] C. Zhao, J. Niu, Y. Zhang, C. Li, P. Hu, *Composites, Part B* **2019**, *178*, 107447.
[129] S. Bairagi, S. W. Ali, *Energy Technol.* **2019**, *7*, 1900538.
[130] J. Liu, B. Yang, L. Lu, X. Wang, X. Li, X. Chen, J. Liu, *Sens. Actuators, A* **2020**, *303*, 111796.
[131] R. S. Sabry, A. D. Hussein, *Polym. Test.* **2019**, *79*, 106001.
[132] X. Guan, B. Xu, J. Gong, *Nano Energy* **2020**, *70*, 104516.
[133] M. Kim, Y. Wu, E. Kan, J. Fan, *Polymers* **2018**, *10*, 745.
[134] A. Sultana, M. M. Alam, A. Biswas, T. R. Middya, D. Mandal, *Transl. Mater. Res.* **2016**, *3*, 045001.
[135] C. M. Guvenc, U. Adem, *J. Alloys Compd.* **2019**, *791*, 674.
[136] B. Jaleh, S. Sodagar, A. Momeni, A. Jabbari, *Mater. Res. Express* **2016**, *3*, 085028.
[137] A. Islam, A. N. Khan, M. F. Shakir, K. Islam, *Mater. Res. Express* **2019**, *7*, 015017.
[138] M. Ando, H. Kawamura, K. Kageyama, Y. Tajitsu, *Jpn. J. Appl. Phys.* **2012**, *51*, 09LD14.
[139] A. Sultana, S. K. Ghosh, V. Sencadas, T. Zheng, M. J. Higgins, T. R. Middya, D. Mandal, *J. Mater. Chem. B* **2017**, *5*, 7352.
[140] W. Wu, S. Bai, M. Yuan, Y. Qin, Z. L. Wang, T. Jing, *ACS Nano* **2012**, *6*, 6231.
[141] Q. Yang, D. Wang, M. Zhang, T. Gao, H. Xue, Z. Wang, Z. Xiong, *J. Alloys Compd.* **2016**, *688*, 1066.
[142] H. H. Fan, C. C. Jin, Y. Wang, H. L. Hwang, Y. F. Zhang, *Ceram. Int.* **2017**, *43*, 5875.
[143] B. Liu, B. Lu, X. Chen, X. Wu, S. Shi, L. Xu, Y. Liu, F. Wang, X. Zhao, W. Shi, *J. Mater. Chem. A* **2017**, *5*, 23634.
[144] E. Yang, Z. Xu, L. K. Chur, A. Behroozfar, M. Baniasadi, S. Moreno, J. Huang, J. Gilligan, M. Minary-Jolandan, *ACS Appl. Mater. Interfaces* **2017**, *9*, 24220.
[145] H. Gao, P. T. Minh, H. Wang, S. Minko, J. Locklin, T. Nguyen, S. Sharma, *Smart Mater. Struct.* **2018**, *27*, 095018.
[146] S. H. Ji, Y.-S. Cho, J. S. Yun, *Nanomaterials* **2019**, *9*, 555.
[147] S. Park, Y. Kwon, M. Sung, B.-S. Lee, J. Bae, W.-R. Yu, *Mater. Des.* **2019**, *179*, 107889.
[148] W. Steinmann, S. Walter, G. Seide, T. Gries, G. Roth, M. Schubnell, *J. Appl. Polym. Sci.* **2011**, *120*, 21.
[149] X.-X. He, J. Zheng, G.-F. Yu, M.-H. You, M. Yu, X. Ning, Y.-Z. Long, *J. Phys. Chem. C* **2017**, *121*, 8663.
[150] T. Lee, C. Chen, C. Tsai, Y. Fuh, *Polymers* **2018**, *10*, 692.
[151] Y. K. Fuh, B. S. Wang, *Nano Energy* **2016**, *30*, 677.
[152] Y.-K. Fuh, J.-C. Ye, P.-C. Chen, H.-C. Ho, Z.-M. Huang, *ACS Appl. Mater. Interfaces* **2015**, *7*, 16923.
[153] Y. K. Fuh, B. S. Wang, C.-Y. Tsai, *Sci. Rep.* **2017**, *7*, 6759.
[154] J. Gui, Y. Zhu, L. Zhang, X. Shu, W. Liu, S. Guo, X. Zhao, *Appl. Phys. Lett.* **2018**, *112*, 072902.
[155] Y.-K. Fuh, P.-C. Chen, H.-C. Ho, Z.-M. Huang, S.-C. Li, *RSC Adv.* **2015**, *5*, 67787.
[156] F.-R. Fan, Z.-Q. Tian, Z. Lin Wang, *Nano Energy* **2012**, *1*, 328.
[157] Z. L. Wang, A. C. Wang, *Mater. Today* **2019**, *30*, 34.
[158] Y. Zi, S. Niu, J. Wang, Z. Wen, W. Tang, Z. L. Wang, *Nat. Commun.* **2015**, *6*, 8376.
[159] A. Yu, Y. Zhu, W. Wang, J. Zhai, *Adv. Funct. Mater.* **2019**, *29*, 1900098.
[160] H. Zou, Y. Zhang, L. Guo, P. Wang, X. He, G. Dai, H. Zheng, C. Chen, A. C. Wang, C. Xu, Z. L. Wang, *Nat. Commun.* **2019**, *10*, 1427.
[161] C. Zhang, L. Zhou, P. Cheng, X. Yin, D. Liu, X. Li, H. Guo, Z. L. Wang, J. Wang, *Appl. Mater. Today* **2020**, *18*, 100496.
[162] R. Cao, J. Wang, S. Zhao, W. Yang, Z. Yuan, Y. Yin, X. Du, N.-W. Li, X. Zhang, X. Li, Z. L. Wang, C. Li, *Nano Res.* **2018**, *11*, 3771.
[163] G. Zhao, S. Gong, H. Wang, J. Ren, N. Wang, Y. Yang, G. Gao, S. Chen, L. Li, *Int. J. Precis. Eng. Manuf.-Green Technol.* **2020**, https://doi.org/10.1007/s40684-020-00246-y.
[164] J.-H. Zhang, Y. Li, X. Hao, *Nanotechnology* **2020**, *31*, 215401.
[165] B. Yu, H. Yu, H. Wang, Q. Zhang, M. Zhu, *Nano Energy* **2017**, *34*, 69.
[166] B. Yu, H. Yu, T. Huang, H. Wang, M. Zhu, *Nano Energy* **2018**, *48*, 464.
[167] J. Shao, X. Chen, X. Li, H. Tian, C. Wang, B. Lu, *Sci. China: Technol. Sci.* **2019**, *62*, 175.
[168] Y. Hu, X. Wang, H. Li, H. Li, Z. Li, *Nano Energy* **2020**, *71*, 104640.
[169] C. K. Chung, K. H. Ke, *Appl. Surf. Sci.* **2020**, *508*, 145310.
[170] S. Megelski, J. S. Stephens, D. B. Chase, J. F. Rabolt, *Macromolecules* **2002**, *35*, 8456.
[171] A. F. Diaz, R. M. Felix-Navarro, *J. Electrostat.* **2004**, *62*, 277.
[172] H. Zou, L. Guo, H. Xue, Y. Zhang, X. Shen, X. Liu, P. Wang, X. He, G. Dai, P. Jiang, H. Zheng, B. Zhang, C. Xu, Z. L. Wang, *Nat. Commun.* **2020**, *11*, 2093.
[173] A. Chen, C. Zhang, G. Zhu, Z. L. Wang, *Adv. Sci.* **2020**, *7*, 2000186.

[174] Z. Qin, Y. Yin, W. Zhang, C. Li, K. Pan, *ACS Appl. Mater. Interfaces* **2019**, *11*, 12452.
[175] T. Huang, C. Wang, H. Yu, H. Wang, Q. Zhang, M. Zhu, *Nano Energy* **2015**, *14*, 226.
[176] T.-H. Kong, S.-S. Lee, G.-J. Choi, I.-K. Park, *ACS Appl. Mater. Interfaces* **2020**, *12*, 17824.
[177] M. Shaikh, Y.-B. Huang, C.-C. Wang, C.-H. Chuang, *Micromachines* **2019**, *10*, 438.
[178] S.-R. Kim, J.-H. Yoo, J.-W. Park, *ACS Appl. Mater. Interfaces* **2019**, *11*, 15088.
[179] S. Cheon, H. Kang, H. Kim, Y. Son, J. Y. Lee, H.-J. Shin, S.-W. Kim, J. H.o Cho, *Adv. Funct. Mater.* **2018**, *28*, 1703778.
[180] G.-J. Choi, S.-H. Baek, S.-S. Lee, F. Khan, J. H. Kim, I.-K. Park, *J. Alloys Compd.* **2019**, *797*, 945.
[181] J.-S. Im, I.-K. Park, *ACS Appl. Mater. Interfaces* **2018**, *10*, 25660.
[182] H. H. Singh, N. Khare, *Energy* **2019**, *178*, 765.
[183] P. Pascariu, I. V. Tudose, C. Pachiu, M. Danila, O. Ioncscu, M. Popescu, E. Koudoumas, M. Suchea, presented at 2018 Int. Semiconductor Conf. (CAS), Sinaia, Romania, October 2018.
[184] Z. Li, M. Zhu, J. Shen, Q. Qiu, J. Yu, B. Ding, *Adv. Funct. Mater.* **2020**, *30*, 1908411.
[185] H.-J. Qiu, W.-Z. Song, X.-X. Wang, J. Zhang, Z. Fan, M. Yu, S. Ramakrishna, Y.-Z. Long, *Nano Energy* **2019**, *58*, 536.
[186] N. Sun, Z. Wen, F. Zhao, Y. Yang, H. Shao, C. Zhou, Q. Shen, K. Feng, M. Peng, Y. Li, X. Sun, *Nano Energy* **2017**, *38*, 210.
[187] C. Jiang, C. Wu, X. Li, Y. Yao, L. Lan, F. Zhao, Z. Ye, Y. Ying, J. Ping, *Nano Energy* **2019**, *59*, 268.
[188] M.-F. Lin, J. Xiong, J. Wang, K. Parida, P. S. Lee, *Nano Energy* **2018**, *44*, 248.
[189] J. Xiong, H. Luo, D. Gao, X. Zhou, P. Cui, G. Thangavel, K. Parida, P. S. Lee, *Nano Energy* **2019**, *61*, 584.
[190] P. Zhao, N. Soin, K. Prashanthi, J. Chen, S. Dong, E. Zhou, Z. Zhu, A. A. Narasimulu, C. D. Montemagno, L. Yu, J. Luo, *ACS Appl. Mater. Interfaces* **2018**, *10*, 5880.
[191] T. Busolo, D. P. Ura, S. K. Kim, M. M. Marzec, A. Bernasik, U. Stachewicz, S. Kar-Narayan, *Nano Energy* **2019**, *57*, 500.
[192] J.-H. Lee, K. Y. Lee, M. K. Gupta, T. Y. Kim, D.-Y. Lee, J. Oh, C. Ryu, W. J. Yoo, C.-Y. Kang, S.-J. Yoon, J.-B. Yoo, S.-W. Kim, *Adv. Mater.* **2014**, *26*, 765.
[193] Y. Zi, L. Lin, J. Wang, S. Wang, J. Chen, X. Fan, P.-K. Yang, F. Yi, Z. L. Wang, *Adv. Mater.* **2015**, *27*, 2340.
[194] X. He, Q. Wen, Y. Sun, Z. Wen, *Nano Energy* **2017**, *40*, 300.
[195] J. He, T. Wen, S. Qian, Z. Zhang, Z. Tian, J. Zhu, J. Mu, X. Hou, W. Geng, J. Cho, J. Han, X. Chou, C. Xue, *Nano Energy* **2018**, *43*, 326.
[196] G. Zhao, X. Zhang, X. Cui, S. Wang, Z. Liu, L. Deng, A. Qi, X. Qiao, L. Li, C. Pan, Y. Zhang, L. Li, *ACS Appl. Mater. Interfaces* **2018**, *10*, 15855.
[197] Y. Wu, J. Qu, W. A. Daoud, L. Wang, T. Qi, *J. Mater. Chem. A* **2019**, *7*, 13347.
[198] P. Sahatiya, S. Kannan, S. Badhulika, *Appl. Mater. Today* **2018**, *13*, 91.
[199] J. Song, B. Yang, W. Zeng, Z. Peng, S. Lin, J. Li, X. Tao, *Adv. Mater. Technol.* **2018**, *3*, 1800016.
[200] Y.-K. Fuh, S.-C. Li, C.-Y. Chen, C.-Y. Tsai, *eXPRESS Polym. Lett.* **2018**, *12*, 136.
[201] X. Wang, B. Yang, J. Liu, Y. Zhu, C. Yang, Q. He, *Sci. Rep.* **2016**, *6*, 36409.
[202] Y. Guo, X.-S. Zhang, Y. Wang, W. Gong, Q. Zhang, H. Wang, J. Brugger, *Nano Energy* **2018**, *48*, 152.
[203] J. Yu, X. Hou, M. Cui, S. Zhang, J. He, W. Geng, J. Mu, X. Chou, *Nano Energy* **2019**, *64*, 103923.

Tugce A. Arica received her B.Sc. (2014) and M.Sc. (2017) in materials science and engineering from the Anadolu University. She is a doctoral student in the Department of Materials Science and Engineering at the İzmir Institute of Technology and she is currently conducting research studies on inorganic nanomaterials.

Tuğba Isık works as a researcher in Mineral Research and Exploration General Directorate at Ankara, Turkey. She received her M.Sc. degree in materials science and engineering in 2015 from İzmir Institute of Technology and her Ph.D. degree in 2019 from the same department. In 2020, she got her M.Sc. in chemistry from University of Bristol, United Kingdom. Her research interest focuses on the fabrication of electrospun nanofibers and their adsorption applications.

Tugrul Guner received his M.Sc. degree in physics at the Izmir Institute of Technology, where he studied quantum mechanics foundations under the supervision of Prof Durmus Ali Demir. Then, he started to study white LEDs, halide perovskites and polymer composites with Prof Mustafa M Demir and he got his Ph.D. degree in materials science and engineering at the same university. He conducts research on the light-matter interactions at the nanoscale regime using time-resolved advanced electron microscopy techniques like Ultrafast TEM.

Nesrin Horzum received a B.Sc. in analytical chemistry from Pamukkkale University, Turkey in 2004. She did her M.Sc. and Ph.D. studies in Department of Chemistry at the Izmir Institute of Technology, Turkey in 2008 and 2013, respectively. During her Ph.D., she joined the Max Planck Institute, Department of Physical Chemistry as a researcher. She is currently an associated professor at the Engineering Sciences Department of Izmir Katip Çelebi University, Turkey. Her current research interests are energy, filtration and sensing applications of polymer-based nanomaterials, as well as smartphone-based sensors for water quality monitoring and biomolecule detection.

Mustafa M. Demir received his B.S. from the Chemistry Department of Boğaziçi University, Turkey in 1999. He did his M.S. and Ph.D. studies in Materials Sciences and Engineering Programme at Sabancı University in 2001 and 2004, respectively. Later he moved to the Max Planck Society Polymer Research Institute in Mainz, Germany as a post-doc researcher under the supervision of Prof. Gerhard Wegner. He is currently a professor at the Izmir Institute of Technology, Department of Materials Science and Engineering. He coordinates an interdisciplinary group working on synthesis and nanotechnologies on soft matter. He has been awarded the "Young researcher" Prize of Turkish Academy of Sciences in 2013.